

Single top production via gluon fusion at CERN LHC

Gad Eilam*

*Technion-Israel Institute of Technology, 32000 Haifa, Israel*Mariana Frank[†] and Ismail Turan[‡]*Department of Physics, Concordia University, 7141 Sherbrooke Street West, Montreal, Quebec, Canada H4B 1R6*

(Received 11 April 2006; published 29 August 2006)

We calculate the one-loop flavor violating top quark decay $t \rightarrow cgg$ in the minimal supersymmetric standard model. We discuss the branching ratios obtained with minimal flavor violation, as well as with soft-supersymmetry induced general flavor violation. Based on this rate we calculate the cross section for the single top quark production via gluon fusion, $gg \rightarrow t\bar{c}$, and evaluate its contribution to the cross section for single top quark production in pp collisions at the Large Hadron Collider. We calculate all contributions coming from the standard model and charged Higgs loops, as well as gluino (and neutralino)-up-type squarks, and chargino-down-type squarks loops. Our numerical results show that the gluino and the chargino contributions are largest over the whole parameter range in the unconstrained minimal supersymmetric standard model. While in general the gluino contributions dominate the cross section, this result depends on the supersymmetric flavor violating parameters in the up and down squark sector, the relative mass of the gauginos, and whether or not the grand unified theory relationships between gaugino masses are satisfied. In the most promising scenarios, the $pp \rightarrow t\bar{c} + \bar{t}c + X$ cross section at the Large Hadron Collider can reach a few hundred fb.

DOI: [10.1103/PhysRevD.74.035012](https://doi.org/10.1103/PhysRevD.74.035012)

PACS numbers: 12.60.Jv, 11.30.Hv, 14.65.Ha

I. INTRODUCTION

One of the main goals at the CERN Large Hadron Collider (LHC) is to study the production and decay of top quarks. The importance of studying the physics of the top is obvious. It is the quark which is closest to the scale of electroweak symmetry breaking and is therefore most sensitive to that scale, and thus to new physics (NP) beyond the standard model (SM). One of the important tests of the SM is its predictions for the yield of single tops in hadronic collisions. The measurement of single top production cross sections has turned out to be a challenging task so far [1] and only upper limits are obtained. For instance, the D0 experiment, at Tevatron II with integrated luminosity of 230 fb^{-1} , obtained the following upper limits on the $s(t)$ -channel processes (as defined below): 6.4 (5.0) pb, at 95% C.L. It is expected that increased luminosity and improved methods of analysis will eventually lead to the detection of single top events in Tevatron II and subsequently at the LHC.

Single top production in hadronic machines has been thoroughly discussed within the SM where, at lowest order, one has the tree level contributions of s -channel ($q\bar{q} \rightarrow t\bar{b}$ through W exchange), t -channel ($ub \rightarrow td$ via W exchange) and $gb \rightarrow tW$ with a top quark exchanged. In [2,3] one finds the most recent SM results, which include next-to-leading order (NLO) corrections. These are predicted to be approximately equal to (all the following cross sections are in pb), 6.6 (4.1) for a single $t(\bar{t})$ production in

the s -channel, and 156 (91) for a single $t(\bar{t})$ production in the t -channel at LHC [2]. The background for single top production in the SM was estimated in [4].

At the same time, there has been an increased interest in studying forbidden or highly suppressed processes as they appear ideal for finding the physics lying beyond the SM. As alluded to before, top quark interactions, in particular, might provide a fertile ground to searches for NP. It is expected that if NP is associated with the mass generation mechanism, it may be more apparent in top quark interactions, rather than in the light fermion sector. Along these lines, there have been suggestions that the flavor changing neutral currents (FCNC) single top quark production could be rather sensitive to non-SM couplings such as tcV ($V = g, \gamma, Z$) and tcH [5]. The advantage in looking for FCNC processes in top physics is that although these exist in the SM, they are minute, leading to tiny, unmeasurable SM effects. In general, any measurable FCNC process involving the top will indicate that one is witnessing the effects of NP. Note that here we are only interested in processes that are driven by FCNC couplings, which are highly suppressed in the SM by the Glashow-Iliopoulos-Maiani (GIM) mechanism. Therefore we do not consider NP corrections to SM couplings (like tbW or Zqq) or the contributions of new particles (either external or internal), like Z' or W' , except those of the supersymmetric partners of SM particles.

FCNC effects in top production contribute to the following single top production processes on the partonic level: $cg \rightarrow t, cg \rightarrow tg, cq(\bar{q}) \rightarrow tq(\bar{q}), q\bar{q} \rightarrow t\bar{c}$ and $gg \rightarrow t\bar{c}$, as well as all the above with $c \rightarrow u$. These subprocesses have been investigated in the presence of FCNC effective couplings and in the framework of various NP models [5].

*Electronic address: eilam@physics.technion.ac.il†Electronic address: mfrank@vax2.concordia.ca‡Electronic address: ituran@physics.concordia.ca

Of all scenarios of physics beyond the SM, supersymmetry is the most popular. A characteristic feature of supersymmetry is that, in addition to the SM FCNC generated by the Cabibbo-Kobayashi-Maskawa (CKM) mixing matrix, it can provide large soft supersymmetry-generated FCNC which would enhance rates and cross sections beyond SM values. The proton collider LHC can produce supersymmetric particles, such as squarks and gluinos, with masses up to 3 TeV; as well as potentially lighter ones, such as charginos/neutralinos. Flavor-changing interactions appear in supersymmetry in loops involving these particles, and thus enhancements in FCNC signals are expected at the LHC.

Single top quark production generated through FCNC processes has been discussed within the effective Lagrangian formalism in a model independent way [6], as well as in model-dependent scenarios [7]. The purpose of this study is to analyze one such class of rare single quark FCNC production: the gluon fusion $gg \rightarrow t\bar{c}$ within the framework of low-energy supersymmetry. This process was analyzed in [8] where QCD-only loops (loops of gluino and squarks), were evaluated in the context of the unconstrained minimal supersymmetric standard model (MSSM). However it is known from analyses of $t \rightarrow cV$ that charginos, and sometimes neutralinos, can have a large effect on FCNC. Here we first discuss the rare decay $t \rightarrow cgg$ and show it to be larger than $t \rightarrow cg$ over most of the parameter space in certain cases. Then we perform a complete analysis of $gg \rightarrow t\bar{c}$ in both the constrained MSSM (where FCNC decays and cross sections are driven by chargino-down-like squark loops) and the unconstrained MSSM (where gluino and neutralino loops contribute as well). We include the SM and charged Higgs contributions, contributions from chargino, neutralinos and gluino loops, as well as interference effects between SM and non-SM effects, in the context of the most general left-left, left-right and right-right intergenerational squark mixings. We also address the observability of these channels at LHC.

Our paper is organized as follows: After a description of the FCNC sources in the unconstrained MSSM (Sec. II), we present our complete analysis of the branching ratio for the top quark $t \rightarrow cgg$ in MSSM, and compare it to the SM case, where $t \rightarrow cgg$ was shown to be larger than $t \rightarrow cg$ [9] (Sec. III). Section IV is devoted to the calculation of the gluon fusion cross section $gg \rightarrow t\bar{c}$, as well as the evaluation of the cross section for $pp \rightarrow t\bar{c} + X$ at the LHC through gluon fusion. We include a detailed numerical analysis of the various relative supersymmetric contributions from gluino and chargino loops with or without grand unified theory (GUT) mass relations, in addition to a comparison of the constrained versus the unconstrained MSSM predictions, as well as observability of these channels. Our conclusions and prospects for experimental observations are presented in Sec. V.

II. FCNC IN THE UNCONSTRAINED MSSM

In the unconstrained MSSM there are two sources of flavor violation. The first one arises from the different mixing of quarks in the d - and u -sectors in the physical bases, and it is described by the CKM matrix (inherited from the SM). In the minimal version of MSSM (the constrained MSSM) this is the only source of flavor violation. The second source of flavor violation consists of a possible misalignment between the rotations that diagonalize the quark and squark sectors, and it is a characteristic of soft supersymmetry breaking. We work in the most general version of the model and discuss the constrained version as a limit. The superpotential of the MSSM Lagrangian is

$$\mathcal{W} = \mu H^1 H^2 + Y_l^{ij} H^1 L^i e_R^j + Y_d^{ij} H^1 Q^i d_R^j + Y_u^{ij} H^2 Q^i u_R^j. \quad (2.1)$$

The part of the soft-SUSY-breaking Lagrangian responsible for the nonminimal squark family mixing is given by

$$\mathcal{L}_{\text{soft}}^{\text{squark}} = -\tilde{Q}^{i\dagger} (M_{\tilde{Q}}^2)_{ij} \tilde{Q}^j - \tilde{u}^{i\dagger} (M_{\tilde{U}}^2)_{ij} \tilde{u}^j - \tilde{d}^{i\dagger} (M_{\tilde{D}}^2)_{ij} \tilde{d}^j + Y_u^i A_u^{ij} \tilde{Q}_i H^2 \tilde{u}_j + Y_d^i A_d^{ij} \tilde{Q}_i H^1 \tilde{d}_j. \quad (2.2)$$

In the above expressions Q is the $SU(2)$ scalar doublet, u, d are the up- and down-quark $SU(2)$ singlets ($\tilde{Q}, \tilde{u}, \tilde{d}$ represent scalar quarks), respectively, $Y_{u,d}$ are the Yukawa couplings and i, j are generation indices. The flavor-changing effects come from the nondiagonal entries in the bilinear terms $M_{\tilde{Q}}^2, M_{\tilde{U}}^2$, and $M_{\tilde{D}}^2$, and from the trilinear terms A_u and A_d . Here $H^{1,2}$ represent two $SU(2)$ Higgs doublets with vacuum expectation values

$$\langle H^1 \rangle = \begin{pmatrix} \frac{v_1}{\sqrt{2}} \\ 0 \end{pmatrix} \equiv \begin{pmatrix} \frac{v \cos \beta}{\sqrt{2}} \\ 0 \end{pmatrix}, \quad \langle H^2 \rangle = \begin{pmatrix} 0 \\ \frac{v_2}{\sqrt{2}} \end{pmatrix} \equiv \begin{pmatrix} 0 \\ \frac{v \sin \beta}{\sqrt{2}} \end{pmatrix}, \quad (2.3)$$

where $v = (\sqrt{2}G_F)^{-1/2} = 246$ GeV, and the angle β is defined by $\tan \beta \equiv v_2/v_1$, the ratio of the vacuum expectation values of the two Higgs doublets and μ is the Higgs mixing parameter.

Since we are concerned with top quark physics, we assume that the non-CKM squark mixing is significant only for transitions between the squarks of the second and third generations. These mixings are expected to be the largest in grand unified models and are also experimentally the least constrained. The most stringent bounds on these transitions come from $b \rightarrow s\gamma$. In contrast, there exist strong experimental bounds involving the first squark generation, based on data from $K^0 - \bar{K}^0$ and $D^0 - \bar{D}^0$ mixing [10].

It is convenient to specify the squark mass matrices in the super-CKM basis, in which the mass matrices of the quark fields are diagonalized by rotating the superfields. Our parametrization of the flavor-nondiagonal squark mass matrices for the up- and down-type squarks, for the MSSM

with real parameters, reads as follows,

$$\mathcal{M}_{\tilde{u}}^2 = \begin{pmatrix} M_{\tilde{L}u}^2 & 0 & 0 & m_u \mathcal{A}_u & 0 & 0 \\ 0 & M_{\tilde{L}c}^2 & (M_{\tilde{U}}^2)_{LL} & 0 & m_c \mathcal{A}_c & (M_{\tilde{U}}^2)_{LR} \\ 0 & (M_{\tilde{U}}^2)_{LL} & M_{\tilde{L}t}^2 & 0 & (M_{\tilde{U}}^2)_{RL} & m_t \mathcal{A}_t \\ m_u \mathcal{A}_u & 0 & 0 & M_{\tilde{R}u}^2 & 0 & 0 \\ 0 & m_c \mathcal{A}_c & (M_{\tilde{U}}^2)_{RL} & 0 & M_{\tilde{R}c}^2 & (M_{\tilde{U}}^2)_{RR} \\ 0 & (M_{\tilde{U}}^2)_{LR} & m_t \mathcal{A}_t & 0 & (M_{\tilde{U}}^2)_{RR} & M_{\tilde{R}t}^2 \end{pmatrix}, \quad (2.4)$$

$$\mathcal{M}_{\tilde{d}}^2 = \begin{pmatrix} M_{\tilde{L}d}^2 & 0 & 0 & m_d \mathcal{A}_d & 0 & 0 \\ 0 & M_{\tilde{L}s}^2 & (M_{\tilde{D}}^2)_{LL} & 0 & m_s \mathcal{A}_s & (M_{\tilde{D}}^2)_{LR} \\ 0 & (M_{\tilde{D}}^2)_{LL} & M_{\tilde{L}b}^2 & 0 & (M_{\tilde{D}}^2)_{RL} & m_b \mathcal{A}_b \\ m_d \mathcal{A}_d & 0 & 0 & M_{\tilde{R}d}^2 & 0 & 0 \\ 0 & m_s \mathcal{A}_s & (M_{\tilde{D}}^2)_{RL} & 0 & M_{\tilde{R}s}^2 & (M_{\tilde{D}}^2)_{RR} \\ 0 & (M_{\tilde{D}}^2)_{LR} & m_b \mathcal{A}_b & 0 & (M_{\tilde{D}}^2)_{RR} & M_{\tilde{R}b}^2 \end{pmatrix}, \quad (2.5)$$

where

$$\begin{aligned} M_{\tilde{L}q}^2 &= M_{\tilde{Q},q}^2 + m_q^2 + \cos 2\beta (T_q - Q_q s_W^2) m_Z^2, & M_{\tilde{R}\{u,c,t\}}^2 &= M_{\tilde{U},\{u,c,t\}}^2 + m_{u,c,t}^2 + \cos 2\beta Q_t s_W^2 m_Z^2, \\ M_{\tilde{R}\{d,s,b\}}^2 &= M_{\tilde{D},\{d,s,b\}}^2 + m_{d,s,b}^2 + \cos 2\beta Q_b s_W^2 m_Z^2, & \mathcal{A}_{u,c,t} &= A_{u,c,t} - \mu \cot \beta, & \mathcal{A}_{d,s,b} &= A_{d,s,b} - \mu \tan \beta, \end{aligned} \quad (2.6)$$

with m_q , T_q , Q_q the mass, isospin, and electric charge of the quark q , m_Z the Z-boson mass, $s_W \equiv \sin \theta_W$ and θ_W the electroweak mixing angle. In the above matrices we assumed that significant mixing occurs between the second and third generations only.

We define the dimensionless flavor-changing parameters $(\delta_{U,D}^{23})_{AB}$ ($AB = LL, LR, RL, RR$) from the flavor off-diagonal elements of the squark mass matrices Eqs. (2.4) and (2.5) in the following way. To simplify the calculation we assume that all diagonal entries in $(M_{\tilde{U}}^2)_{LL}$, $(M_{\tilde{U}}^2)_{LR}$, $(M_{\tilde{U}}^2)_{RL}$ and $(M_{\tilde{U}}^2)_{RR}$ and similarly for $(M_{\tilde{D}}^2)_{AB}$, are set equal to the common value M_{SUSY}^2 , and then we normalize the off-diagonal elements to M_{SUSY}^2 [11,12],

$$\begin{aligned} (\delta_{\tilde{U}}^{ij})_{LL} &= \frac{(M_{\tilde{U}}^2)_{LL}^{ij}}{M_{\text{SUSY}}^2}, & (\delta_{\tilde{D}}^{ij})_{LL} &= \frac{(M_{\tilde{D}}^2)_{LL}^{ij}}{M_{\text{SUSY}}^2} & (\delta_{\tilde{U}}^{ij})_{RR} &= \frac{(M_{\tilde{U}}^2)_{RR}^{ij}}{M_{\text{SUSY}}^2}, & (\delta_{\tilde{D}}^{ij})_{RR} &= \frac{(M_{\tilde{D}}^2)_{RR}^{ij}}{M_{\text{SUSY}}^2} & (\delta_{\tilde{U}}^{ij})_{LR} &= \frac{(M_{\tilde{U}}^2)_{LR}^{ij}}{M_{\text{SUSY}}^2}, \\ (\delta_{\tilde{D}}^{ij})_{LR} &= \frac{(M_{\tilde{D}}^2)_{LR}^{ij}}{M_{\text{SUSY}}^2} & (\delta_{\tilde{U}}^{ij})_{RL} &= \frac{(M_{\tilde{U}}^2)_{RL}^{ij}}{M_{\text{SUSY}}^2}, & (\delta_{\tilde{D}}^{ij})_{RL} &= \frac{(M_{\tilde{D}}^2)_{RL}^{ij}}{M_{\text{SUSY}}^2} & (i \neq j, i, j = 2, 3). \end{aligned} \quad (2.7)$$

The matrix $\mathcal{M}_{\tilde{u}}^2$ can further be diagonalized by an additional 6×6 unitary matrix Γ_U to give the up squark mass eigenvalues

$$(\mathcal{M}_{\tilde{u}}^2)^{\text{diag}} = \Gamma_U^\dagger \mathcal{M}_{\tilde{u}}^2 \Gamma_U. \quad (2.8)$$

For the down squark mass matrix, we also can define $\mathcal{M}_{\tilde{d}}^2$ as the similar form of Eq. (2.8) with the replacement of $(M_{\tilde{U}}^2)_{AB}$ ($A, B = L, R$) by $(M_{\tilde{D}}^2)_{AB}$. Note that while $SU(2)_L$ gauge invariance implies that $(M_{\tilde{U}}^2)_{LL} = K_{\text{CKM}} (M_{\tilde{D}}^2)_{LL} K_{\text{CKM}}^\dagger$, the matrices $(M_{\tilde{U}}^2)_{LL}$ and $(M_{\tilde{D}}^2)_{LL}$ are correlated. Since the connecting equations are rather complicated and contain several unknown parameters, we proceed by including the flavor changing parameters $(\delta_{U,D}^{ij})_{AB}$

as independent quantities, while restricting them using previously set bounds [10].

Thus, in the super-CKM basis, there are potentially new sources of flavor-changing neutral currents: Chargino-quark-squark couplings, neutralino-quark-squark coupling and gluino-quark-squark coupling, which arise from the off-diagonal elements of $(M_{\tilde{U},\tilde{D}}^2)_{LL}$, $(M_{\tilde{U},\tilde{D}}^2)_{LR}$ and $(M_{\tilde{U},\tilde{D}}^2)_{RR}$. Previous considerations of flavor violating decays [13] in the MSSM have shown that both up and down squarks contribute significantly. Our analysis shows that this is the case here too, and which one is dominant depends on the parameters of the model, and, in particular, on the relative mass hierarchy between the chargino and the gluino.

In the super-CKM basis, the quark-up squark-gluino (\tilde{g}) interaction is given by

$$\mathcal{L}_{u\tilde{u}\tilde{g}} = \sum_{i=1}^3 \sqrt{2} g_s T_{st}^r [\tilde{u}_i^s(\Gamma_U)^{ia} P_L \tilde{g}^r \tilde{u}_a^t - \tilde{u}_i^s(\Gamma_U)^{(i+3)a} P_R \tilde{g}^r \tilde{u}_a^t + \text{H.c.}], \quad (2.9)$$

where T^r are the $SU(3)_c$ generators, $P_{L,R} \equiv (1 \mp \gamma_5)/2$, $i = 1, 2, 3$ is the generation index, $a = 1, \dots, 6$ is the scalar quark index, and s, t are color indices. In the gluino interaction, the flavor changing effects from soft broken terms $M_{\tilde{Q}}^2$, $M_{\tilde{U}}^2$ and A_u on the observables are introduced through the matrix Γ_U .

The relevant Lagrangian terms for the quark-down squark-chargino ($\tilde{\chi}_\sigma^\pm$) interaction are given by

$$\begin{aligned} \mathcal{L}_{u\tilde{d}\tilde{\chi}^+} = & \sum_{\sigma=1}^2 \sum_{i,j=1}^3 \{ \tilde{u}_i [V_{\sigma 2}^* (Y_u^{\text{diag}} K_{\text{CKM}})_{ij}] P_L \tilde{\chi}_\sigma^+ (\Gamma_D)^{ja} \tilde{d}_a \\ & - \tilde{u}_i [g U_{\sigma 1} (K_{\text{CKM}})_{ij}] P_R \tilde{\chi}_\sigma^+ (\Gamma_D)^{ja} \tilde{d}_a \\ & + \tilde{u}_i [U_{\sigma 2} (K_{\text{CKM}} Y_d^{\text{diag}})_{ij}] P_R \tilde{\chi}_\sigma^+ (\Gamma_D)^{(j+3)a} \tilde{d}_a \} \\ & + \text{H.c.} \end{aligned} \quad (2.10)$$

where the index σ refers to chargino mass eigenstates. $Y_{u,d}^{\text{diag}}$ are the diagonal up- and down-quark Yukawa couplings, and V, U are the usual chargino rotation matrices defined by $U^* M_{\tilde{\chi}^\pm} V^{-1} = \text{diag}(m_{\tilde{\chi}_1^\pm}, m_{\tilde{\chi}_2^\pm})$. The flavor changing effects arise from both the off-diagonal elements in the CKM matrix K_{CKM} and from the soft supersymmetry breaking terms in Γ_D .

Finally, the relevant Lagrangian terms for the quark-up squark neutralino ($\tilde{\chi}_n^0$) interaction are

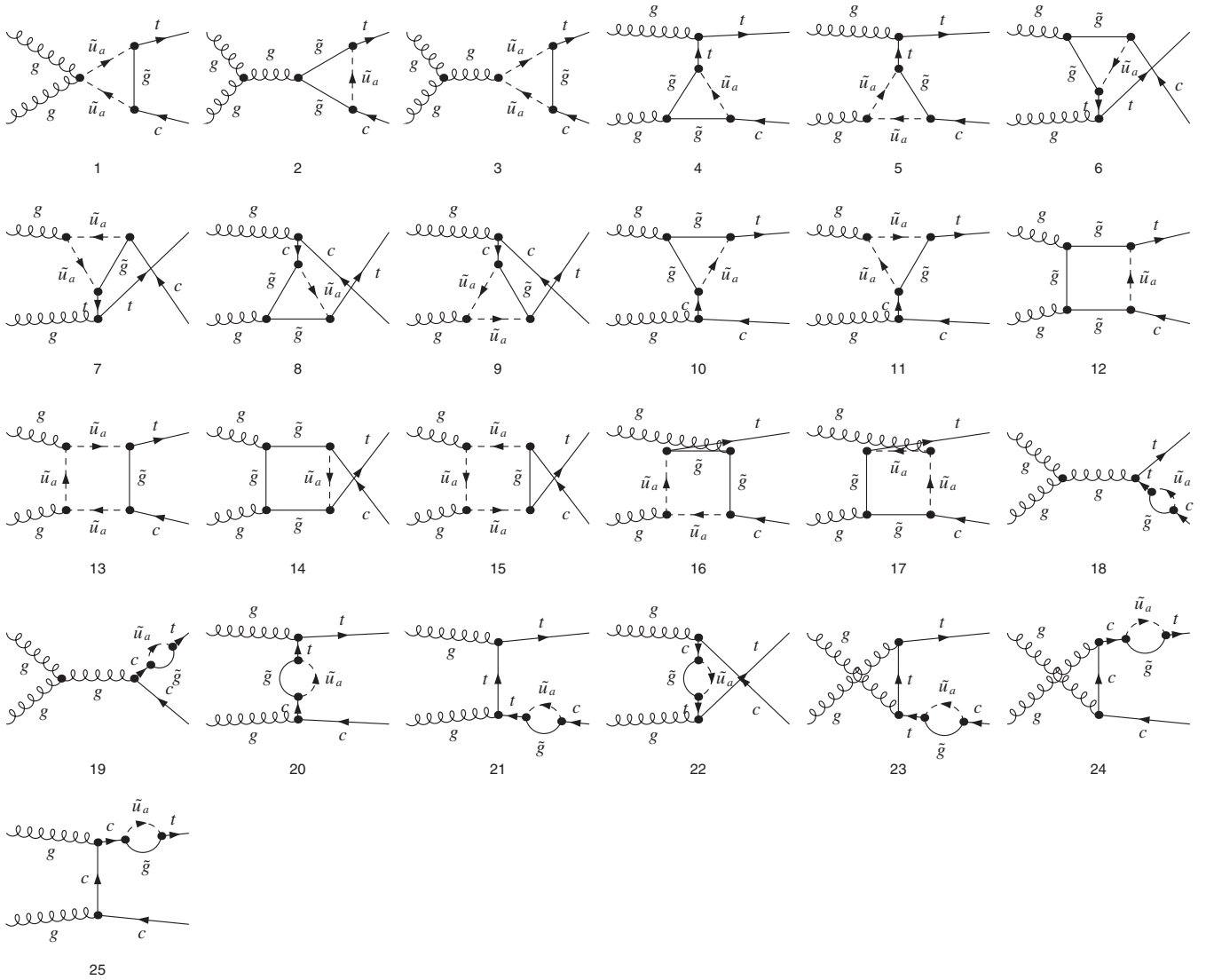


FIG. 1. The one-loop gluino contributions to $gg \rightarrow t\bar{c}$ in the unconstrained MSSM in the 't Hooft-Feynman gauge.

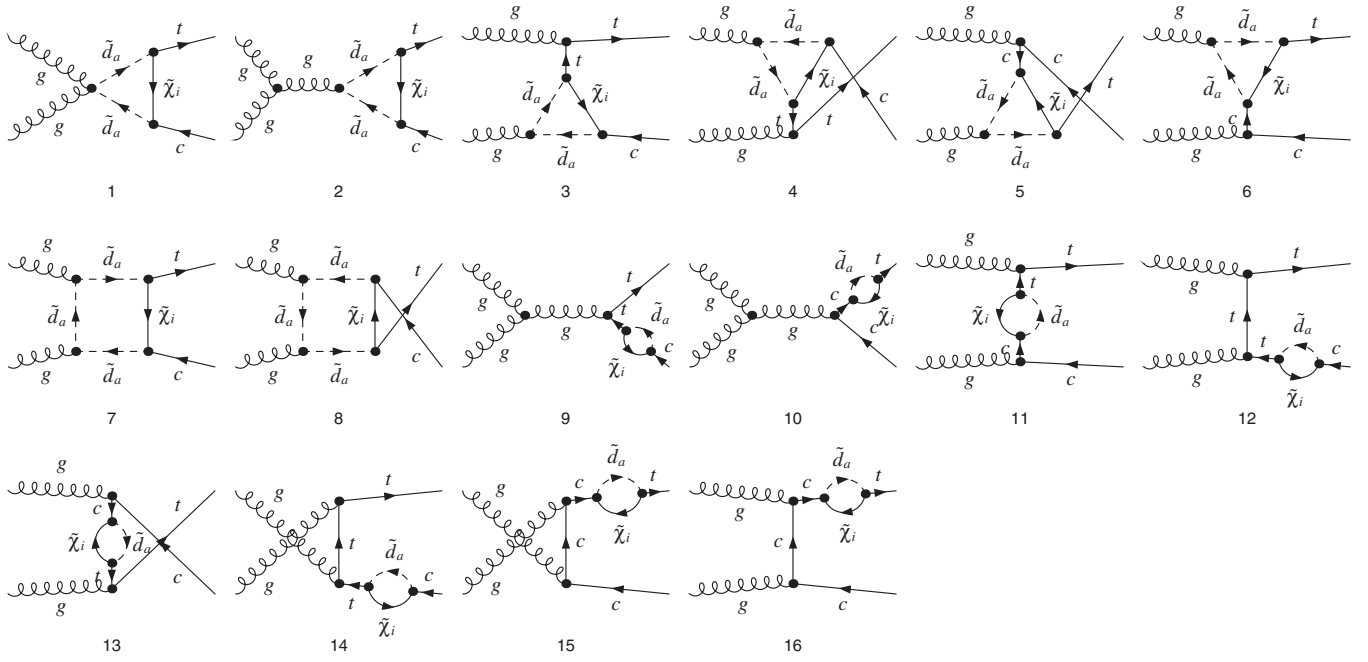


FIG. 2. The one-loop chargino contributions to $gg \rightarrow t\bar{c}$ in the unconstrained MSSM in the 't Hooft-Feynman gauge.

$$\begin{aligned}
\mathcal{L}_{u\bar{u}\tilde{\chi}^0} = & \sum_{n=1}^4 \sum_{i=1}^3 \left\{ \bar{u}_i N_{n1}^* \frac{4}{3} \frac{g}{\sqrt{2}} \tan\theta_W P_L \tilde{\chi}_n^0 (\Gamma_U)^{(i+3)a} \tilde{u}_a \right. \\
& - \bar{u}_i N_{n4}^* Y_u^{\text{diag}} P_L \tilde{\chi}_n^0 (\Gamma_U)^{ia} \tilde{u}_a \\
& - \bar{u}_i \frac{g}{\sqrt{2}} \left(N_{n2} + \frac{1}{3} N_{n1} \tan\theta_W \right) P_R \tilde{\chi}_n^0 (\Gamma_U)^{ia} \tilde{u}_a \\
& \left. - \bar{u}_i N_{n4} Y_u^{\text{diag}} P_R \tilde{\chi}_n^0 (\Gamma_U)^{(i+3)a} \tilde{u}_a \right\}, \quad (2.11)
\end{aligned}$$

where N is the 4×4 rotation matrix which diagonalizes the neutralino mass matrix $M_{\tilde{\chi}^0}$, $N^* M_{\tilde{\chi}^0} N^{-1} = \text{diag}(m_{\tilde{\chi}_1^0}, m_{\tilde{\chi}_2^0}, m_{\tilde{\chi}_3^0}, m_{\tilde{\chi}_4^0})$. As in the gluino case, FCNC terms arise only from supersymmetric parameters in Γ_U .

Most of the previous analyses of FCNC processes in the MSSM concentrated on the mass insertion approximation [14]. In this formalism, the (δ) terms represent mixing between chirality states of different squarks, and it is possible to compute the contributions of the first order flavor changing mass insertions perturbatively, if one assumes smallness of the intergenerational mixing elements $(\delta$'s) when compared with the diagonal elements. However, when the off-diagonal elements in the squark mass matrix become large, the mass insertion approximation is no longer valid [11, 12]. In the general mass eigenstate formalism, the mass matrix in Eq. (2.8) (and the similar one in the down-sector) is diagonalized and the flavor changing parameters enter into our expressions through the matrix $\Gamma_{U,D}$. So, in the rare top decays $t \rightarrow cgg$, the new flavor changing neutral currents show themselves in both gluino-squark-quark and neutralino-squark-quark couplings in the up-type squark loops and in the chargino-squark-quark coupling in the down-type squark

loops. Therefore here, as in our previous work [15], we use the general mass eigenstate formalism as described above.

III. $t \rightarrow cgg$ VERSUS $t \rightarrow cg$ IN MSSM

We present here the comparative analysis of the rare two and three body top quark decays, $t \rightarrow cgg$ and $t \rightarrow cg$, closely following the discussion in our earlier paper [9]. There, we have shown that, within the SM framework, the branching ratio of $t \rightarrow cgg$ is about 2 orders of magnitude larger than that of $t \rightarrow cg$ in SM, a phenomenon which can be dubbed ‘‘higher order dominance’’, and which was revealed e.g., in b and c -physics in the past. For the detailed discussion, see [9] and the relevant references therein. Even though the branching ratio for $t \rightarrow cgg$ dominates the one for the two body decay $t \rightarrow cg$, it is of the order of 10^{-9} and still too small to be detected in collider experiments. Any experimental signal for such decay would indicate physics beyond the SM. So, our aim in this section is to extend the discussion in [9] to a favorable beyond SM framework in which we would expect larger contributions due to extra sources of FCNC—the unconstrained MSSM. Note that we include the SM contributions as well in our calculations.

The one-loop Feynman diagrams contributing to $t \rightarrow cgg$ in the MSSM are given in a set of diagrams Figs. 1–5 in the 't Hooft-Feynman gauge ($\xi = 1$) representing gluino, chargino, neutralino, Higgs, and ghost contributions, respectively.¹ We did not show the SM diagrams here

¹Note that we display the one-loop diagrams for the process $gg \rightarrow t\bar{c}$. The diagrams for the decay can be easily obtained by crossing.

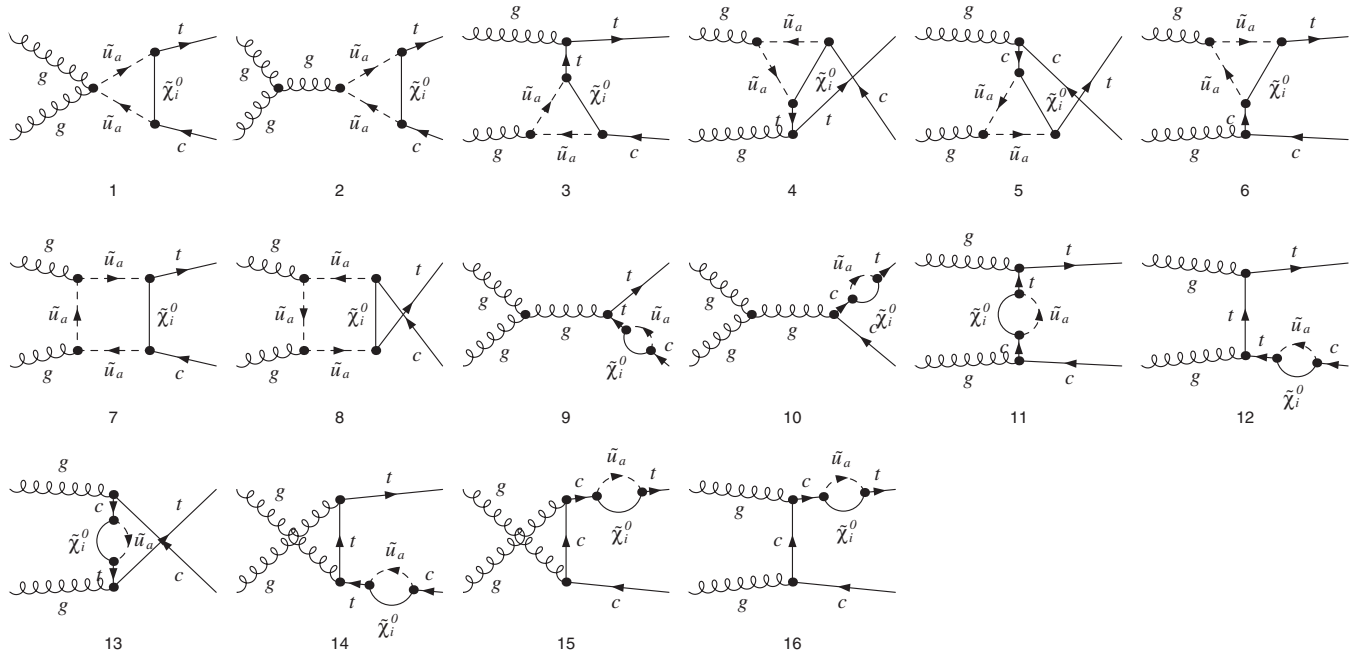


FIG. 3. The one-loop neutralino contributions to $gg \rightarrow t\bar{c}$ in the unconstrained MSSM in the 't Hooft-Feynman gauge.

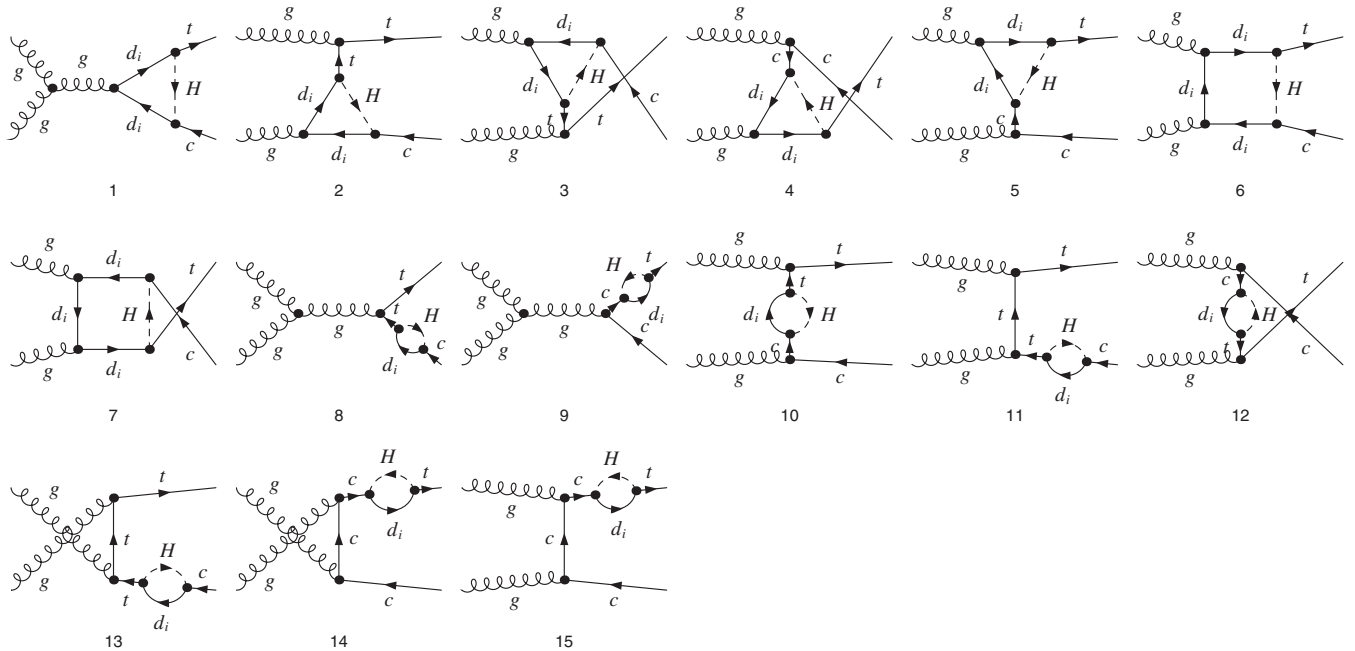


FIG. 4. The one-loop charged Higgs contributions to $gg \rightarrow t\bar{c}$ in the unconstrained MSSM in the 't Hooft-Feynman gauge.

(since they appear in [9]) but we took them into account in the numerical evaluation, for both the decays and the production mode.

As in [9], we choose to use the 't Hooft-Feynman gauge in which the gluon polarization sum is $\sum_{\lambda} \epsilon_{\mu}^*(k, \lambda) \epsilon_{\nu}(k, \lambda) = -g_{\mu\nu}$. In order to obey unitarity, this simple choice results in the existence of QCD ghost

fields whose contributions are shown in Fig. 5. We closely follow the method outlined in [9] and references therein for handling the ghost diagrams.

Divergences inherent in the $t \rightarrow cgg$ calculation are ultraviolet, infrared, and collinear types [9]. In numerical evaluations, we used the softwares FEYNARTS, FORMCALC, and LOOPTOOLS [16] to obtain our results. In addition to

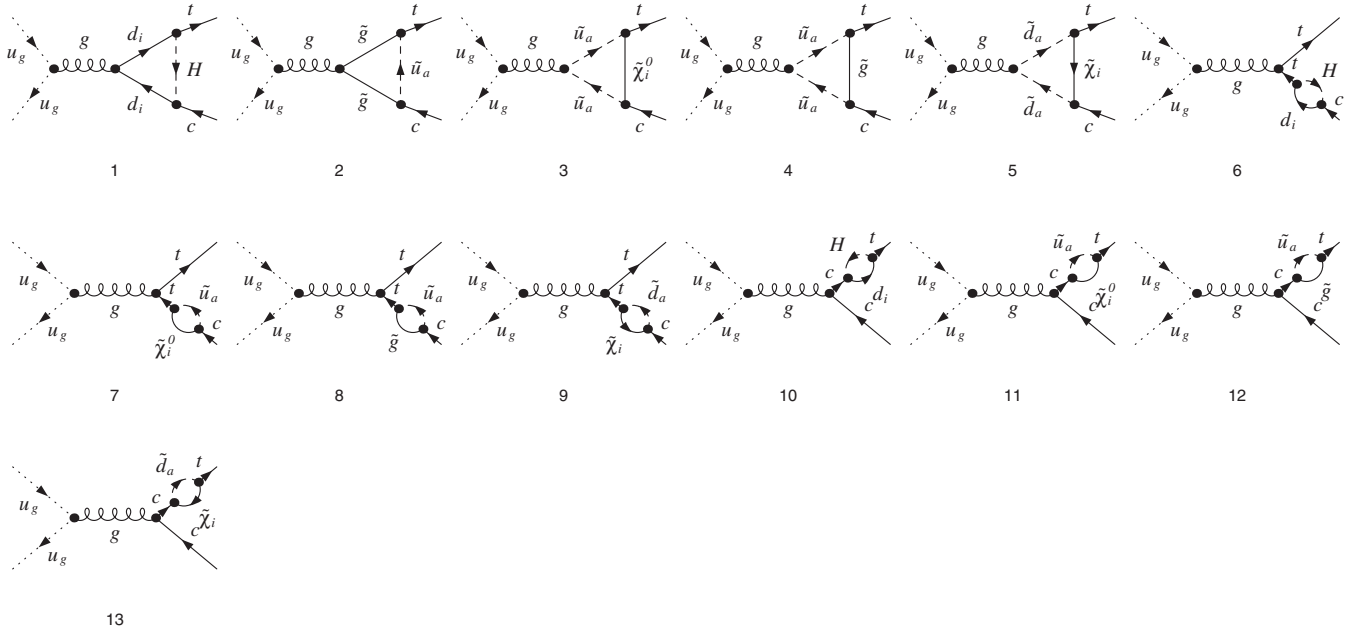


FIG. 5. The one-loop QCD ghost contributions to $gg \rightarrow t\bar{c}$ in the unconstrained MSSM in the 't Hooft-Feynman gauge.

these, HADCALC [17] is used for deriving the pp process corresponding to the gg fusion discussed in the next section. Using utilities offered by FORMCALC, we checked ultraviolet finiteness of our results numerically, and introduced phase space cuts to avoid infrared and collinear singularities.²

Having mentioned some qualitative features of the decay $t \rightarrow cgg$, we do not present here most of the analytical intermediate results. We do this since the calculations are lengthy and uninspiring. Furthermore, we use well known programs.³ We have also checked our calculations with similar ones, whenever published, as we discuss in the next section.

We express the matrix element squared $|\mathcal{M}|^2$ as a sum over the various contributions. These include the SM contribution as given in our previous work [9]. From Figs. 1–5, we obtain expressions for the following non-SM terms: the gluino contribution, chargino, neutralino, charged Higgs and finally the contribution of the ghosts.

The results were expressed in terms of Passarino-Veltman functions [19]. Numerical evaluations of these functions have been carried out with LOOPTOOLS, which does not require reduction of Passarino-Veltman functions to the scalars A_0 , B_0 , C_0 and D_0 . The analytical expressions are obtained with the use of FEYNALC [20].

²These cuts lead to some uncertainties in our results. A more precise approach requires full consideration of the next-to-leading order corrections to $t \rightarrow cg$, similar to the ones in b decays [18].

³The complete analytical results can be obtained by contacting one of us (I.T.)

The partial width $d\Gamma$ for the decay $t \rightarrow cgg$ is given as

$$\begin{aligned}
 d\Gamma(t \rightarrow cgg) &= \frac{1}{2m_t} \sum_{\text{spins}} |\mathcal{M}|^2 d\Phi_3(k_1; k_2, k_3, k_4) d\Phi_3 \\
 &\times (k_1; k_2, k_3, k_4) \\
 &= \frac{d^3k_2}{(2\pi)^3 2k_2^0} \frac{d^3k_3}{(2\pi)^3 2k_3^0} \frac{d^3k_4}{(2\pi)^3 2k_4^0} \\
 &\times (2\pi)^4 \delta^{(4)}(k_1 - k_2 - k_3 - k_4), \quad (3.1)
 \end{aligned}$$

where $k_1(k_2)$ is the momentum of the top (charm) quark and k_3, k_4 the momenta of the gluon pair. The volume element can further be expressed as

$$d\Phi_3(k_1; k_2, k_3, k_4) = \frac{1}{32\pi^3} \int_{(k_3^0)^{\min}}^{(k_3^0)^{\max}} dk_3^0 \int_{(k_2^0)^{\min}}^{(k_2^0)^{\max}} dk_2^0, \quad (3.2)$$

where the limits are

$$\begin{aligned}
 (k_2^0)^{\min} &= \max\left[Cm_t, \frac{\sigma - |\mathbf{k}_3|}{2} \right], \\
 (k_2^0)^{\max} &= \frac{\sigma + |\mathbf{k}_3|}{2} (1 - 2C), \\
 (k_3^0)^{\min} &= Cm_t, \\
 (k_3^0)^{\max} &= \frac{m_t}{2} (1 - 2C),
 \end{aligned} \quad (3.3)$$

with $\sigma = m_t - k_3^0$. In addition, C is the cutoff parameter, chosen nonzero to avoid infrared and collinear singularities [9]. For the numerical calculations in the rest of our study we fix $C = 0.1$, which is large enough to be able to reach the jet energy resolution sensitivity of the LHC detector.

TABLE I. The parameters used in the numerical calculation.

$\alpha_s(m_t)$	$\alpha(m_t)$	$\sin\theta_W(m_t)$	$m_c(m_t)$	$m_b(m_t)$	$m_t(m_t)$
0.106 829	0.007 544	0.22	0.63 GeV	2.85 GeV	174.3 GeV

The results are sensitive to the choice of the C parameter; we find that by decreasing C to 0.01, $\text{BR}(t \rightarrow cgg)$ can increase by a factor of 2–4.

The total decay width of the top quark is taken to be $\Gamma_t = 1.55$ GeV. The parameters used in our numerical evaluation are given in Table I.

The MSSM parameters M_{SUSY} , M_2 , m_{A^0} , μ , A , and $\tan\beta$ are chosen as free for the constrained MSSM and the SUSY-GUT mass relations are assumed.⁴ (This is the first scenario we consider). Inclusion of the flavor violating parameters δ 's among second and third generation squarks (the unconstrained MSSM) adds eight more free parameters. Imposing SUSY-GUT relations favors a heavy gluino, which decreases the gluino contributions for both processes under consideration, $t \rightarrow cg(g)$ and $gg \rightarrow t\bar{c}$, and which enhances chargino contributions, since the lightest chargino becomes much lighter than gluino.

As a second scenario we consider the constrained and unconstrained MSSM without imposing SUSY-GUT relations. In this case, we run the $U(1)$ gaugino mass parameter M_1 and the gluino mass $M_{\tilde{g}}$ separately.⁵ Thus the two scenarios we concentrate on are MSSM with, and MSSM without, SUSY-GUT relations.

Given the still large number of parameters in either of these scenarios, the parameter space needs to be reduced by making further assumptions. So, for simplicity, we assume that the soft SUSY-breaking parameters in the squark sector are set to the common value M_{SUSY} . In addition to this, the trilinear linear terms A_{u_i} and A_{d_i} are chosen to be real and equal to each other and μ is also taken to be real and positive.

In the case of flavor violating MSSM, only the mixing between the second and the third generations is turned on, and the dimensionless parameters δ 's run over as much of the interval (0,1) as allowed.⁶ The allowed upper limits of δ 's are constrained by the requirement that $m_{\tilde{u}_i, \tilde{d}_i} > 0$ and consistent with the experimental lower bounds (depending on the chosen values of M_{SUSY} , A , $\tan\beta$, and μ). We assume a lower bound of 96 GeV for all up squark masses

⁴The existence of a GUT theory at Planck scale leads to relations among gaugino mass parameters of the form

$$M_1 = (5s_W^2/3c_W^2)M_2 = (5\alpha/3c_W^2\alpha_s)m_{\tilde{g}}$$

where α and α_s are running coupling constants.

⁵We still keep the relation between M_1 and M_2 , rather than fixing them independently, since this does not affect significantly the final results.

⁶Even though δ 's are allowed to be negative, we run them in the positive region.

and 90 GeV for the down squark masses [21]. The Higgs masses are calculated with FEYNHIGGS [22], with the requirement that the lightest neutral Higgs mass is larger than 114 GeV. Other experimental bounds included are [21]: 96 GeV for the lightest chargino, 46 GeV the lightest neutralino, and 195 GeV for the gluino. Throughout the paper, only m_{A^0} and A are fixed globally in the decay and production separately, $m_{A^0} = 400$ GeV and $A = 620$ GeV in the decay process $t \rightarrow cgg$ (and $t \rightarrow cg$ as well) and $m_{A^0} = 500$ GeV and $A = 400$ GeV, respectively, in the single top production process $gg \rightarrow t\bar{c}$.

The rest of the section is devoted to the presentation of our results for the three body decay $t \rightarrow cgg$ and the comparison with the two body channel $t \rightarrow cg$, both within the MSSM framework. Since the flavor violating parameters δ 's play very important role in both decays (both are flavor-violating rare top decay channels), we vary them by keeping only a single flavor off-diagonal element nonzero unless otherwise stated. In this section, $\tan\beta = 10$ is chosen in all figures except for Fig. 8, where the dependence of the BR's on $\tan\beta$ are shown. Furthermore, the common SUSY scale $M_{\text{SUSY}} = 300$ GeV; $M_2 = 200$ GeV, and $\mu = 200$ GeV are chosen and fixed globally in this section. Since we are only interested in the relative size of the $\text{BR}(t \rightarrow cgg)$ with respect to $\text{BR}(t \rightarrow cg)$, we consider the scenario of MSSM with GUT gaugino mass relations for illustration purposes, and present the case without GUT mass relations in one figure at the end of the section, namely, Fig. 9.

Figure 6 shows the branching ratios of the decays $t \rightarrow cgg$ and $t \rightarrow cg$ as functions of $(\delta_D^{23})_{LL}$ on the left panel, and as functions of $(\delta_D^{23})_{LR} = (\delta_D^{23})_{RL}$ on the right panel. Since the flavor off-diagonal δ 's in the up sector are switched off, these figures show chargino-only contributions. As seen from the panels, $\text{BR}(t \rightarrow cgg)$ is almost 2 orders of magnitude larger than $\text{BR}(t \rightarrow cg)$ in most of the parameter space, and especially for small δ_D^{23} , up to $\delta_D^{23} \sim 0.4$. As δ_D^{23} 's become larger, $\text{BR}(t \rightarrow cg)$ increases rapidly and becomes larger than $\text{BR}(t \rightarrow cgg)$ for $(\delta_D^{23})_{LL} \geq 0.6$ for the left panel and for $(\delta_D^{23})_{LR} \geq 0.8$ for the right panel. The maximum value reached is around 10^{-7} for nonzero $(\delta_D^{23})_{LL}$ and 10^{-8} for the special case $(\delta_D^{23})_{LR} = (\delta_D^{23})_{RL}$. (Note that $t \rightarrow cg$ can get even larger in this part of the phase space). These two figures demonstrate explicitly that $t \rightarrow cgg$ is larger than $t \rightarrow cg$ over most of the parameter space. We have checked the dependence of $\text{BR}(t \rightarrow cgg)$ and $\text{BR}(t \rightarrow cg)$ on $(\delta_D^{23})_{RR}$ and observed that $\text{BR}(t \rightarrow cgg)$ remains 2 orders of magnitude larger than $\text{BR}(t \rightarrow cg)$ for the most part of the interval, while the sensitivity to $(\delta_D^{23})_{RR}$ variations is not as pronounced as in the (depicted) LL and LR, RL cases. In this case, $\text{BR}(t \rightarrow cg)$ can reach a few times 10^{-9} .

In Fig. 7, the $(\delta_U^{23})_{LL}$ and $(\delta_U^{23})_{RR}$ dependence of the branching ratios of $t \rightarrow cgg$ and $t \rightarrow cg$ decays are shown on the left and right panels, respectively. Since the GUT

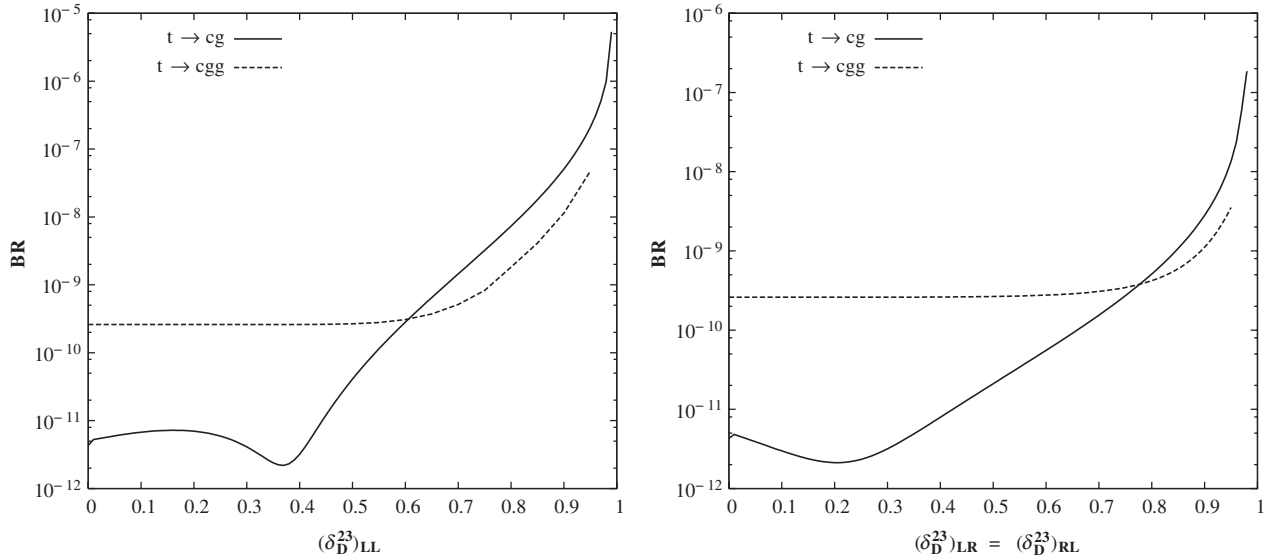


FIG. 6. Left panel: Branching ratios of $t \rightarrow cgg$ and $t \rightarrow cg$ decays as functions of $(\delta_D^{23})_{LL}$ with the assumption that GUT relations hold. Right panel: Branching ratios as functions of $(\delta_D^{23})_{LR} = (\delta_D^{23})_{RL}$ under the same conditions. The parameters are chosen as $\tan\beta = 10$, $M_{\text{SUSY}} = 300$ GeV, $M_2 = \mu = 200$ GeV.

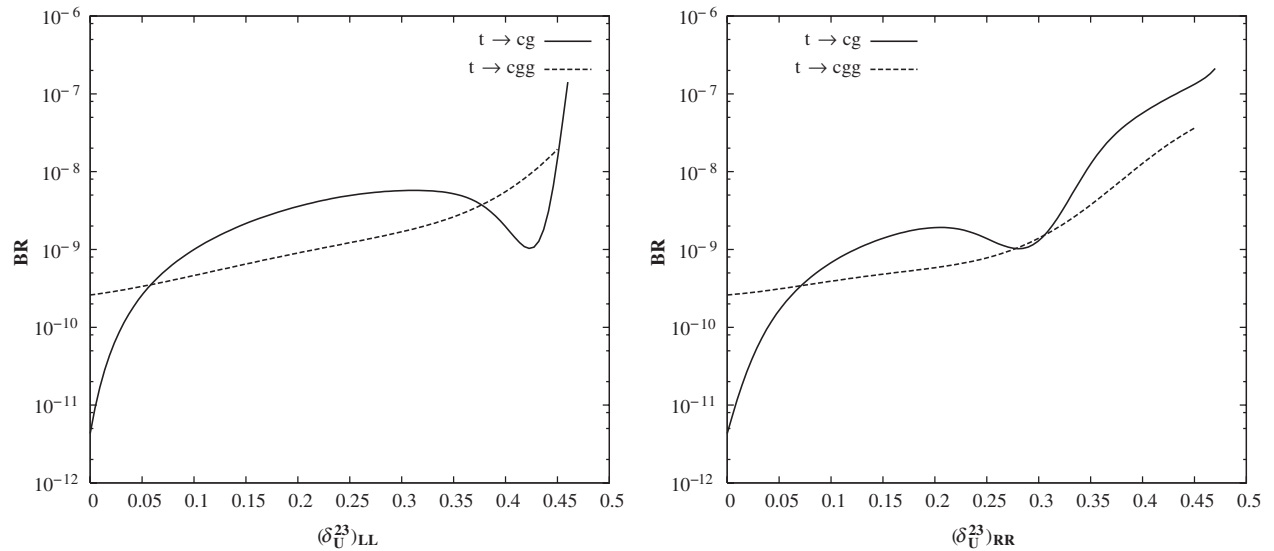


FIG. 7. Left panel: Branching ratios of $t \rightarrow cgg$ and $t \rightarrow cg$ decays as functions of $(\delta_U^{23})_{LL}$ with the assumption that GUT relations hold. Right panel: Branching ratios as functions of $(\delta_U^{23})_{RR}$ under the same conditions. The parameters are chosen as $\tan\beta = 10$, $M_{\text{SUSY}} = 300$ GeV, $M_2 = \mu = 200$ GeV.

relations are assumed to hold, the gluino mass is rather heavy, about 600 GeV, when M_2 is chosen as 200 GeV. The 2 orders of magnitude difference between the BR's for the flavor conserving MSSM disappear once we introduce a small flavor violation (~ 0.1) between the second and third generations in the up squark sector, which holds for either LL or RR case. The branching ratio of $t \rightarrow cg$ exceeds that of $t \rightarrow cgg$ for $\delta_U^{23} \geq 0.1$. The maximum attainable branching ratio for $t \rightarrow cg$ is around 10^{-7} , and for $t \rightarrow cgg$, 10^{-8} – 10^{-7} which represents 2 orders of

magnitude enhancement for $t \rightarrow cgg$, and more than 4 orders of magnitude enhancement for $t \rightarrow cg$, with respect to the constrained case. The case of $(\delta_U^{23})_{LR} = (\delta_U^{23})_{RL}$ is very similar to the case with nonzero $(\delta_U^{23})_{LL}$ (left panel) or $(\delta_U^{23})_{RR}$ (right panel).

Figure 8 shows the $\tan\beta$ dependence of the decays with zero flavor off-diagonal parameters $\delta = 0$ for $M_{\text{SUSY}} = 300$ GeV, $M_2 = \mu = 200$ GeV. For the decay $t \rightarrow cgg$, the SUSY contribution comes from the chargino sector in the MSSM (there are no gluino or neutralino contribu-

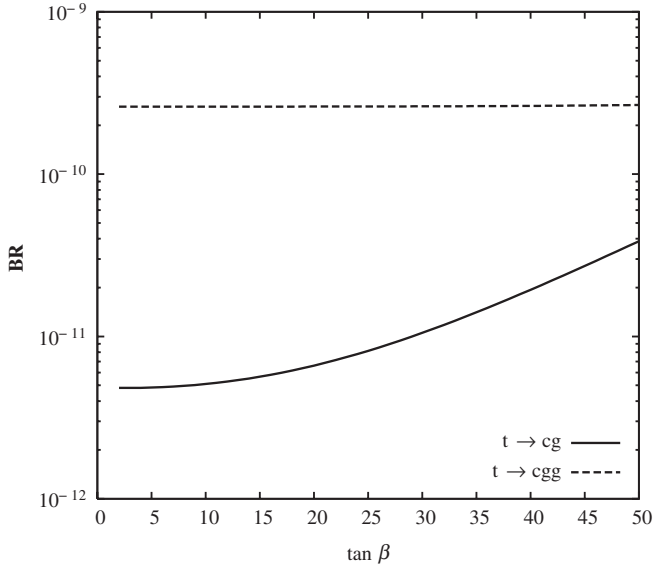


FIG. 8. The branching ratios of $t \rightarrow cgg$ and $t \rightarrow cg$ decays as functions of $\tan\beta$ with the assumption that GUT relations hold. It is further assumed that all flavor off-diagonal parameters δ 's are zero in both the up and down sectors (constrained MSSM). The other parameters are chosen as $M_{\text{SUSY}} = 300$ GeV, $M_2 = \mu = 200$ GeV.

tions.) Overall the SM contribution dominates over the MSSM one and the $\tan\beta$ dependence is insignificant, as expected, since the constrained MSSM gives smaller contributions than the SM to FCNC decays at one-loop level. There is a mild dependence on $\tan\beta$ for $t \rightarrow cg$ decay in the very large $\tan\beta$ region (≥ 25). In addition to that, we analyzed the case with nonzero δ 's as well and, for example, for $(\delta_U^{23})_{LL} = 0.4$, we obtain $\text{BR}(t \rightarrow cgg)$ almost 2

orders of magnitude larger than $\text{BR}(t \rightarrow cg)$ in the entire $\tan\beta$ interval considered.

The last figure of the section, Fig. 9, presents the dependence of the branching ratios on the SUSY flavor-violating parameters in the MSSM without SUSY-GUT relations. For illustration, we present the $(\delta_U^{23})_{LL}$ dependence of the BR's for the gluino mass $m_{\tilde{g}} = 200$ GeV on the left panel, and for $m_{\tilde{g}} = 300$ GeV on the right panel. The other parameters are chosen the same as before, $M_{\text{SUSY}} = 300$ GeV, $M_2 = \mu = 200$. As seen from the figure, the relative difference between the decays not only disappears immediately after switching $(\delta_U^{23})_{LL}$ on (more precisely, for $(\delta_U^{23})_{LL} \geq 0.01$) but also $t \rightarrow cg$ exceeds $t \rightarrow cgg$ with a constant factor of 5. This is a gluino dominated case which favors the two-body decay $t \rightarrow cg$ over the three body decay. The decay $t \rightarrow cg$ can get as large as 10^{-5} for $m_{\tilde{g}} = 200$ GeV and 10^{-6} for $m_{\tilde{g}} = 300$ GeV.

From the analysis in this section, it is fair to say that the branching ratio for the three body $t \rightarrow cgg$ decay dominates largely over the one for the two body $t \rightarrow cg$ mode for the flavor conserving MSSM scenario with SUSY-GUT relations, and remains larger even if nonzero flavor off-diagonal parameters in the down squark sector are turned on. Such dominance is valid only for relatively small flavor violating parameter in the up squark sector ($(\delta_U^{23})_{LL} < 0.1$). Our results here show that the $t \rightarrow cgg$ channel gives a larger contribution (and may be easier to access) than the $t \rightarrow cg$ channel over most of the parameter space if the flavor violation originated from the down squark sector.

The predictions of the constrained MSSM (without intergenerational squark mixings) are similar to the SM ones. Thus the existence of such SUSY FCNC mixings, directly related to the SUSY breaking mechanism, is crucial for the enhancement of the branching ratios.

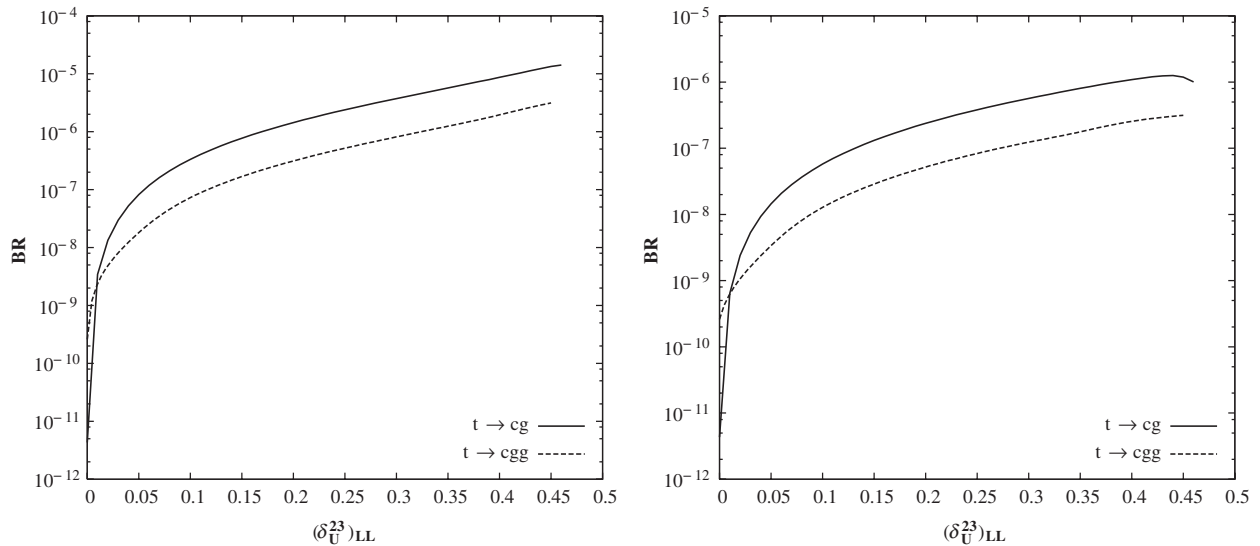


FIG. 9. The branching ratios of $t \rightarrow cgg$ and $t \rightarrow cg$ decays as functions of $(\delta_U^{23})_{LL}$ without GUT relations for $m_{\tilde{g}} = 200$ GeV, on the left panel, and $m_{\tilde{g}} = 300$ GeV, on the right panel. The parameters are chosen as $\tan\beta = 10$, $M_{\text{SUSY}} = 300$ GeV, $M_2 = \mu = 200$ GeV.

Another motivation for considering $t \rightarrow cgg$ is the issue of single top quark production, which is one of today's challenging task at colliders. If $t \rightarrow cgg$ is a promising channel with respect to $t \rightarrow cg$,⁷ the next question would be what are the consequences of this for the single top quark searches at colliders. For this purpose, $gg \rightarrow t\bar{c} + \bar{t}c$ needs to be considered. Gluons will become very important and abundant at the LHC, which reaches very high energies. Therefore, the rest of the paper is devoted to the consideration of the $pp \rightarrow t\bar{c} + \bar{t}c + X$ cross section at LHC, within the flavor-violating MSSM, by assuming only the gluon fusion contribution at partonic level.

IV. $pp \rightarrow t\bar{c} + \bar{t}c + X$ AT LHC

Having discussed the decay mode $t \rightarrow cgg$ and shown that it is a more promising signal than $t \rightarrow cg$ in the previous section, we consider here the top-charm associated production via gluon fusion $gg \rightarrow t\bar{c} + \bar{t}c$ at the partonic level. Since, at the LHC, TeV or even higher-scale energies are going to be probed, gluons inside the proton will become very important. This process, as well as other channels involving light quarks, has been considered by Liu *et al.* [8] in the unconstrained MSSM driven by SUSY-QCD contributions only. Their results show clearly that $t\bar{c}$ production through gluon fusion is the dominant channel over the ones involving light quarks $q\bar{q}'$, $q, q' = u, c, d, s$. For example, 87% of the total hadronic cross section $\sigma(pp \rightarrow t\bar{c} + \bar{t}c + X)$ comes from the partonic channel $gg \rightarrow t\bar{c} + \bar{t}c$ for $(\delta_U^{23})_{LL,RR} = 0.7$ [8]. We agree with their results presented in [8] once we make the required modifications to the input parameters.

Here, we present the complete calculation of the hadronic cross section $\sigma(pp \rightarrow t\bar{c} + \bar{t}c + X)$ at LHC by including all one-loop contributions. In addition to the gluino, the chargino, neutralino, and charged Higgs loops as well as the SM part is included. The full set of Feynman diagrams contributing to the process at one-loop level through gluino, chargino, neutralino, and Higgs loops is given, respectively, in Figs. 1–4 in the 't Hooft-Feynman gauge. As mentioned in the previous section, we did not display here the SM diagrams available in our previous paper [9] for the $t \rightarrow cgg$ decay case. Note that, as mentioned before, working in the 't Hooft-Feynman gauge for this process requires the inclusion of QCD ghost diagrams, represented in Fig. 5.

The partonic level differential cross section for $gg \rightarrow t\bar{c}$ can be expressed as

$$d\hat{\sigma} = \frac{1}{32\pi^2 \hat{s}^{3/2}} |p|_{\text{out}} |\mathcal{M}|^2 d\Omega_3, \quad (4.1)$$

$$|p|_{\text{out}}^2 = \frac{(\hat{s} + m_t^2)^2}{4\hat{s}} - m_t^2$$

⁷The observability of $t \rightarrow cgg$ at LHC will be briefly discussed at the end of Sec. IV.

where Ω_3 is the angular volume of the third particle and $\sqrt{\hat{s}}$ is the partonic center of mass energy.⁸ The matrix squared $|\mathcal{M}|^2$ can be calculated by using the expressions, for $t \rightarrow cgg$ by simply using the *crossing symmetry* (see for example [23]). Then, the hadronic cross section is obtained by convoluting the partonic cross section with the parton distribution functions (PDF's), $f_{g/p}$. So, the total hadronic cross section reads

$$\sigma = \int_{\xi_0}^1 d\xi \frac{d\mathcal{L}}{d\xi} \hat{\sigma}(\xi s, \alpha_s(\mu_R)) \quad (4.2)$$

where $\hat{\sigma}(\xi s, \alpha_s(\mu_R))$ is the total partonic cross section at the center of mass energy $\sqrt{\hat{s}} = \sqrt{\xi s}$ (\sqrt{s} is the hadronic center of mass energy) depending on the renormalization scale μ_R . Here ξ_0 defines the production threshold of the process. The parton luminosity is defined as

$$\frac{d\mathcal{L}}{d\xi} = \int_{\xi}^1 \frac{dx}{x} f_{g/p}(x, \mu_F) f_{g/p}(\xi/x, \mu_F) \quad (4.3)$$

where μ_F is the factorization scale, which is assumed to be equal to the renormalization scale μ_R in our numerical analysis. If one needs to sum over all possible partonic subprocesses contributing to the particular final state, there will be a sum over PDF's in Eq. (4.3).

We assume that the top quark in the final state will be reconstructed from events and thus it is a physical observable. Of course, to identify the hadronic final state requires making a series of cuts on the transverse momentum p_T of the top and charm quarks, the rapidity η , and the jet separation ΔR_{34} . The following set is used for the cuts

$$p_{T_c}, p_{T_t} \geq 15 \text{ GeV} \quad \eta_c, \eta_t \leq 2.5 \quad \Delta R_{34} \geq 0.4. \quad (4.4)$$

Their effect is translated into cuts on the limits of ξ in the calculation of the partonic cross section. For the transformation of the initial partons to initial hadrons, the program HADCALC [17] was used, incorporating the Les Houche Accord Parton Density Function library (LHAPDF) version 4.2 [24] with the recent data set CTEQ6AB [25].

For the numerical calculations, we have chosen as input parameter the values $m_{A^0} = 500 \text{ GeV}$, $A = 400 \text{ GeV}$. In addition the hadronic center of mass energy $\sqrt{s} = 14 \text{ GeV}$ is taken for the LHC. The factorization and renormalization scales are chosen as the production threshold of the process ($\mu_F = \mu_R = 174.93 \text{ GeV}$).

We discuss the dependence of the total hadronic cross section of $gg \rightarrow t\bar{c} + \bar{t}c$ process, $\sigma(pp \rightarrow t\bar{c} + \bar{t}c + X)$, on various MSSM parameters for certain δ values in scenarios with and without GUT relations. Note that for simplicity we assume a common δ parameter in the up

⁸For simplicity we assumed m_c zero in our analytical, but not in numerical, estimates.

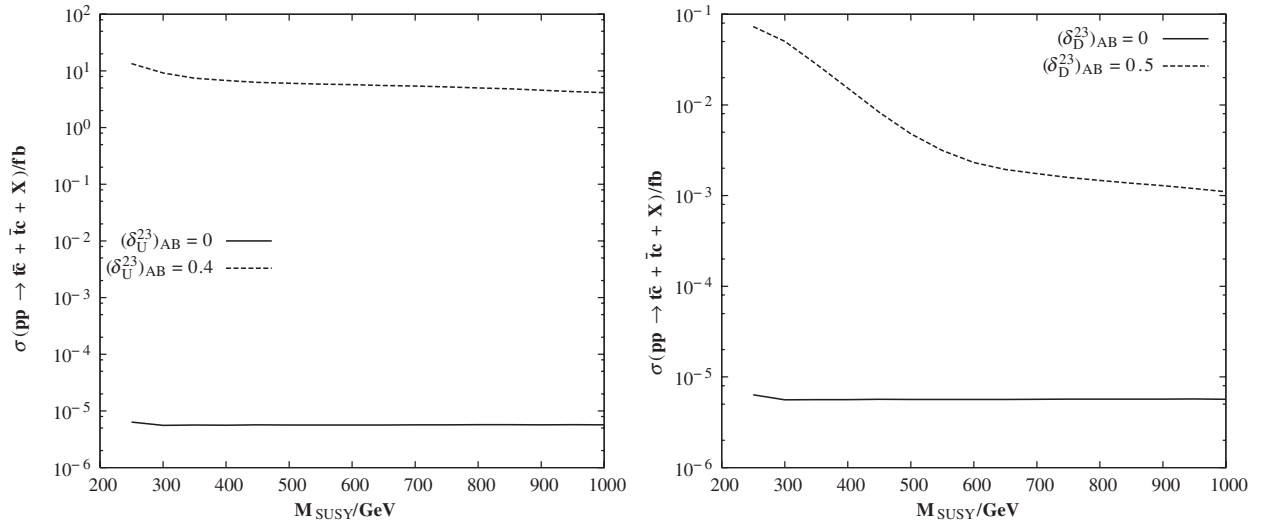


FIG. 10. The total hadronic cross section $\sigma(pp \rightarrow t\bar{c} + \bar{t}c + X)$ via gluon fusion as a function of M_{SUSY} for $\tan\beta = 5$, $\mu = 250$ GeV, $M_2 = 200$ GeV, and $m_{\tilde{g}} = 300$ GeV. On the left panel, $\delta_U^{23} = 0.4$ is chosen and compared with the constrained MSSM case $\delta_U^{23} = 0$. The same is shown on the right panel for $\delta_D^{23} = 0.5$.

and down sector $(\delta_{U,D}^{23})_{LL} = (\delta_{U,D}^{23})_{RR} = (\delta_{U,D}^{23})_{LR} = (\delta_{U,D}^{23})_{RL}$ and only one (U or D) nonzero at a time. At the end of this section we discuss the relative magnitude of the contributions coming from the gluino, chargino, and the rest.

Figure 10 shows the M_{SUSY} dependence of the total hadronic cross section $\sigma(pp \rightarrow t\bar{c} + \bar{t}c + X)$ for $\tan\beta = 5$, $\mu = 250$ GeV, $M_2 = 200$ GeV, and $m_{\tilde{g}} = 300$ GeV. On the left panel, there are two curves, for $(\delta_U^{23})_{AB} = 0$, and 0.4. The cross section depends very weakly on M_{SUSY} and, for the constrained MSSM case, the SM contribution is the dominant one. There is an enhancement of more than

6 orders of magnitude in the unconstrained MSSM over the constrained one, and the cross section can be as large as 15 fb for $(\delta_U^{23})_{AB} = 0.4$. In the down sector, shown on the right panel, the sensitivity of σ to M_{SUSY} is quite strong, and there is an enhancement of about 2 orders of magnitude in the interval 250–1000 GeV. There are still 2–4 orders of magnitude difference between the constrained MSSM versus the unconstrained MSSM scenarios at $(\delta_D^{23})_{AB} = 0.5$. The maximum cross section is around 0.1 fb at around $M_{\text{SUSY}} \sim 250$ GeV.

In Fig. 11, on the left panel, the total cross section $\sigma(pp \rightarrow t\bar{c} + \bar{t}c + X)$ is shown as a function of the gluino

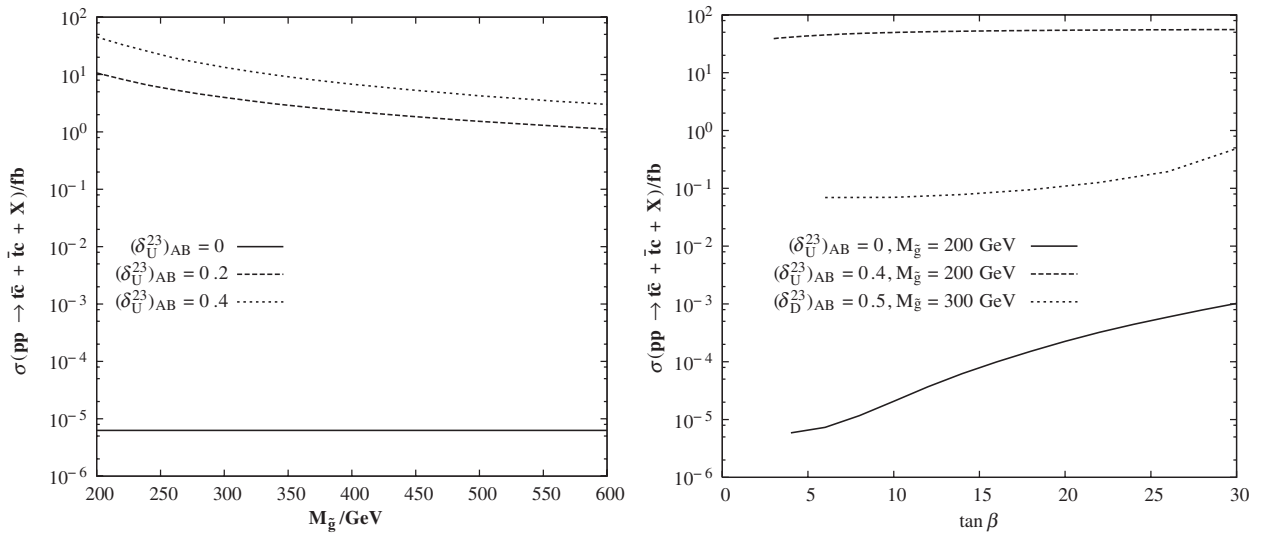


FIG. 11. On the left panel, the total hadronic cross section $\sigma(pp \rightarrow t\bar{c} + \bar{t}c + X)$ via gluon fusion as a function of $m_{\tilde{g}}$ for $\tan\beta = 5$, $M_{\text{SUSY}} = \mu = 250$ GeV, and $M_2 = 200$ GeV at various $(\delta_U^{23})_{AB}$, $A, B = L, R$. On the right panel, $\sigma(pp \rightarrow t\bar{c} + \bar{t}c + X)$ as a function of $\tan\beta$ at various $\delta_{U,D}^{23}$ and $m_{\tilde{g}}$ values.

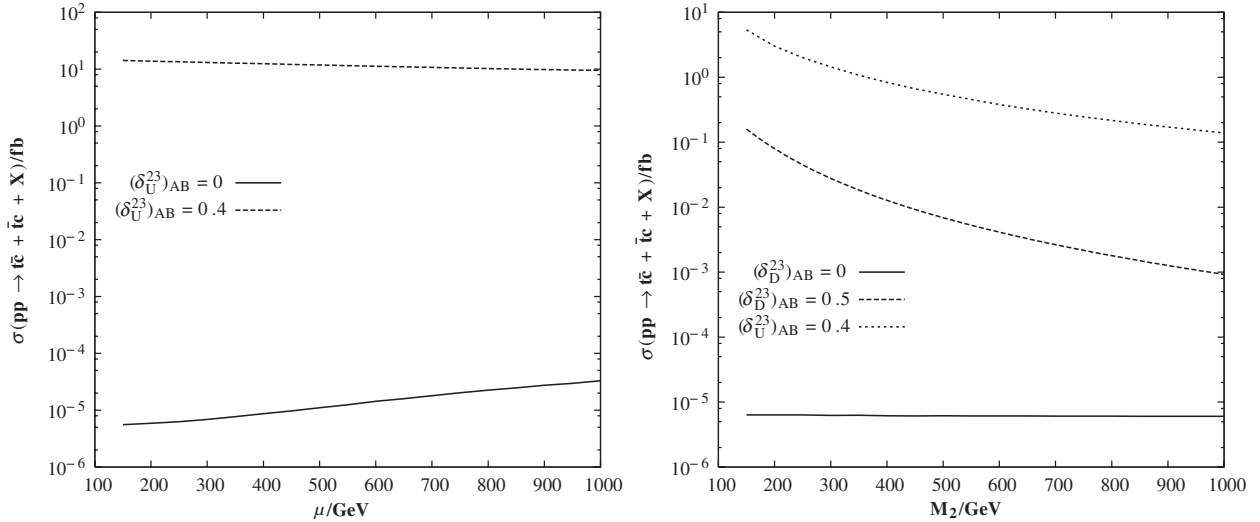


FIG. 12. On the left panel, the total hadronic cross section $\sigma(pp \rightarrow t\bar{c} + \bar{t}c + X)$ via gluon fusion as a function of μ for $\tan\beta = 5$, $M_{\text{SUSY}} = 250$ GeV, $M_2 = 200$ GeV, and $m_{\tilde{g}} = 300$ GeV at various $(\delta_{U,D}^{23})_{AB}$, $A, B = L, R$. On the right panel, $\sigma(pp \rightarrow t\bar{c} + \bar{t}c + X)$ as a function of M_2 at various $(\delta_{U,D}^{23})_{AB}$ with GUT mass relations.

mass for various $(\delta_{U,D}^{23})_{AB}$ values. Again the constrained MSSM case is dominated by the SM contribution, while for the unconstrained MSSM, $\sigma \sim 45$ fb for $m_{\tilde{g}} = 200$ GeV and $(\delta_{U,D}^{23})_{AB} = 0.4$, which is more than 7 orders of magnitude larger than for the case with $(\delta_{U,D}^{23})_{AB} = 0$. On the right panel, the $\tan\beta$ dependence of the total cross section is shown for $\mu = 250$ GeV, $M_2 = 200$ GeV, and $m_{\tilde{g}} = 200, 300$ GeV ($(\delta_{U,D}^{23})_{AB} = 0, 0.4$ and $(\delta_{D}^{23})_{AB} = 0.5$). For very large $\tan\beta$ values, the cross section reaches 0.001 fb in the constrained MSSM, while in the unconstrained case, for $(\delta_{U,D}^{23})_{AB} = 0.4$ and $m_{\tilde{g}} = 200$ GeV, a cross section of 60 fb is obtained. For $(\delta_{U,D}^{23})_{AB} = 0.5$ and $m_{\tilde{g}} = 300$ GeV, the cross section under these conditions reaches a few fb.

Figure 12 illustrates the μ (on the left panel) and M_2 (on the right panel) dependences of the total hadronic cross section σ for representative values of $(\delta_{U,D}^{23})_{AB}$. The parameters are $\tan\beta = 5$, $M_{\text{SUSY}} = 250$ GeV, $M_2 = 200$ GeV, and $m_{\tilde{g}} = 300$ GeV for the left panel, and $\tan\beta = 5$, $M_{\text{SUSY}} = \mu = 250$ GeV, and $m_{\tilde{g}} = 300$ GeV for the right panel. For nonzero $(\delta_{U,D}^{23})_{AB}$, the cross section σ is not sensitive to μ and remains around 15 fb, but it decreases significantly with M_2 in the interval $M_2 \in [150-1000]$ GeV, if there is a nonzero δ in either the up or down sector. The cross section ranges between 10 fb to 0.1 fb for $M_2 = 150$ GeV and 1000 GeV, respectively, for $(\delta_{U,D}^{23})_{AB} = 0.4$, and between 0.1 fb to 0.001 fb for $(\delta_{D}^{23})_{AB} = 0.5$.

Before concluding, we comment on the relative contributions of the gluino, chargino, and the rest (namely, neutralino, charged Higgs, and SM contributions) to the total cross section. In Table II, we show the relative contributions to $\sigma(pp \rightarrow t\bar{c} + \bar{t}c + X)$ from gluino, chargino, and the rest, in the MSSM with GUT mass relations (the case without GUT mass relations is shown for $m_{\tilde{g}} =$

300 GeV in brackets if different). For simplicity we set $(\delta_{U,D}^{23})_{AB} = (\delta_{D}^{23})_{AB}$, $A, B = L, R$, and the values 0, 0.2, and 0.4 are considered. The other parameters are $A = 400$ GeV, $\tan\beta = 10$, $M_{\text{SUSY}} = \mu = 250$ GeV and $M_2 = 200$ GeV. The case in which no GUT relations between gaugino masses are imposed corresponds (in our analysis) to the case in which the gluino mass is allowed to be smaller. This is the reason why only the gluino contributions are enhanced in this scenario. The gluino contributions are also dominant for the case in which GUT relations are imposed, and the chargino contributions are 2 orders of magnitude smaller. However, one could envisage a case in which the SUSY FCNC parameters $(\delta_{D}^{23})_{AB}$ are allowed to be large, while the ones in the up sector restricted to be small or zero, in which the chargino contribution could be dominant. In the case of the constrained MSSM only chargino loops contribute.

So far, we have considered a common flavor violation in the LL, LR, RL, and RR sectors of sfermion matrix. However, one could analyze the relative effects of flavor violation in each sector and determine how large their

TABLE II. Relative contributions to the total cross section $\sigma(pp \rightarrow t\bar{c} + \bar{t}c + X)$, in fb, with and without GUT mass relations. $(\delta_{U,D}^{23})_{AB} = (\delta_{D}^{23})_{AB} = 0, 0.2, 0.4$, $A, B = L, R$ is considered. The rest of the parameters are $A = 400$ GeV, $\tan\beta = 10$, $M_{\text{SUSY}} = \mu = 250$ GeV and $M_2 = 200$ GeV. For the case without GUT, $m_{\tilde{g}} = 300$ GeV is used and $(\delta_{U,D}^{23})_{AB}$ are given in brackets.

$(\delta_{U,D}^{23})_{AB} = (\delta_{D}^{23})_{AB}$	0	0.2 (No GUT)	0.4 (No GUT)
Gluino loop	0	1.09 (4.05)	3.07 (14.13)
Chargino loop	1.7710^{-5}	0.0052	0.034
The rest	6.1010^{-6}	0.0025	0.017

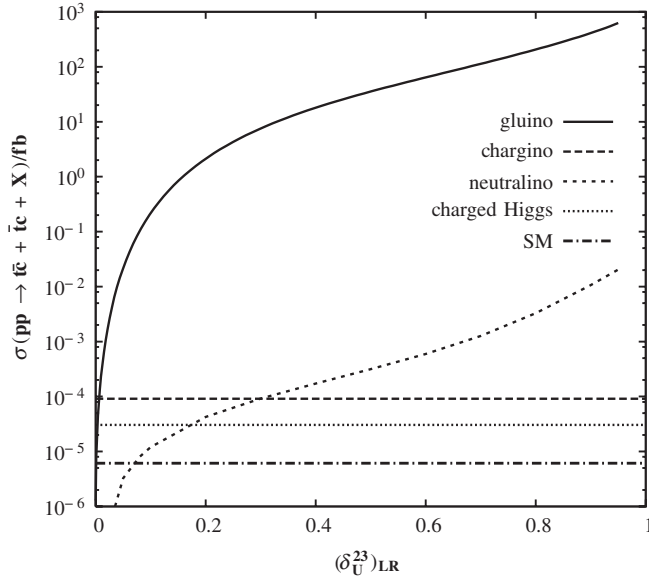


FIG. 13. The total hadronic cross section $\sigma(pp \rightarrow t\bar{c} + \bar{t}c + X)$ via gluon fusion as a function of $(\delta_U^{23})_{LR}$ (other flavor violating parameters are assumed zero) for $\tan\beta = 30$, $m_{A^0} = 500$ GeV, $A = 300$ GeV, $\mu = M_{\text{SUSY}} = 400$ GeV, $M_2 = 200$ GeV, and $m_{\tilde{g}} = 200$ GeV.

contribution to the cross section could be. If the flavor violation comes only from the up sector, then $(\delta_U^{23})_{LR}$ is the most sensitive parameter, as shown in Fig. 13 where we took the parameter values $m_{A^0} = 500$ GeV, $\mu = M_{\text{SUSY}} = 400$ GeV, $A = 300$ GeV, $m_{\tilde{g}} = 200$ GeV, and $\tan\beta = 30$. Of course this is only one of the best possible scenarios. As seen from the figure, the total cross section can be as big as 630 fb and the gluino contribution becomes dominant if there exist a large flavor violation in the up LR sector between the second and third generations. If the flavor violation comes only from the down sector, $(\delta_D^{23})_{LL}$ gives the largest contributions. In this case the cross section is dominated by chargino contribution and can be as large as 0.4 fb with the same parameter values.

Finally, we would like to qualitatively comment on the observability of both the decay and the production channels of the top quark considered here. The rare decay $t \rightarrow cgg$ can in general be treated twofold way: one can either treat it inclusively with $t \rightarrow cg$ or consider it as a separate channel. The former means that $t \rightarrow cgg$ is taken as QCD-correction to $t \rightarrow cg$ by assuring that two of three final state jets are collinear so that only two can be resolved in the detector. The latter can be a competitive possibility if $\text{BR}(t \rightarrow cgg)$ is significantly larger than that of $t \rightarrow cg$. In here, and in our previous work [9], we conclude that $t \rightarrow cgg$ could be potentially more significant than the two-body decay channel in the SM [9] and in some part of the MSSM parameter space. However, this should be taken with a dose of caution. Collinearity should be avoided by applying certain cuts. The unphysical C -parameter introduced in the phase space here plays an essential role to

distinguish $t \rightarrow cg$ from $t \rightarrow cgg$. Even though in our explorations we considered several values of C , C must be taken in the range of jet energy resolution of the upcoming LHC detector. For $C \ll 0.1$, $t \rightarrow cgg$ dominates over $t \rightarrow cg$ for a larger parameter space, thus availability of better jet resolution would give an opportunity to detect $t \rightarrow cgg$ before $t \rightarrow cg$.

At LHC, predominantly $t\bar{t}$ pairs are produced. If we consider one of the top quarks decay mainly as $t \rightarrow bW$ and the other one exotically as $t \rightarrow cgg$, then the signal would be $pp \rightarrow t\bar{t} \rightarrow (l\nu)ggc\bar{b}$ (4-jets, a lepton and missing energy), where $l = e, \mu$.⁹ For the single lepton plus jet topology, it is possible to reconstruct the final state fully, and the b -quark can be tagged to obtain a cleaner signal, which introduces extra selection efficiency. We assume $\sigma(pp \rightarrow t\bar{t}) = 800$ pb at LHC and also that the W boson decays leptonically, not hadronically. Under this conditions, one can calculate roughly the total expected (raw) number of events as

$$N = \sigma(pp \rightarrow t\bar{t}) \times \text{BR}(\bar{t} \rightarrow \bar{b}W) \times \text{BR}(W \rightarrow l\nu) \\ \times L \times \text{BR}(t \rightarrow cgg),$$

where L is the integrated luminosity which we take as 100 fb^{-1} . Therefore we have $N = 800 \times 10^3 \times 1 \times (2/9) \times 100 \times \text{BR}(t \rightarrow cgg) = (1.77 \times 10^7) \times \text{BR}(t \rightarrow cgg)$. So, one expects around $(1.8 \times 10^7) \times \text{BR}(t \rightarrow cgg)$ lepton + 4 jets events for an integrated luminosity 100 fb^{-1} . However, counting a total efficiency including trigger efficiency, selection efficiency, as well as detector geometrical acceptance, one would approximate a total efficiency around 1% [26]. Thus, the number reduces to $(1.8 \times 10^5) \times \text{BR}(t \rightarrow cgg)$. So, if the flavor violation comes from the down squark sector, then for most part of the parameter space $t \rightarrow cgg$ would dominate over $t \rightarrow cg$ by around 2 orders of magnitude, but both will remain unobserved because lepton + jets events are less than a single event. If the flavor violation comes from up-squark sector, then $t \rightarrow cg$ dominates and can reach 10^{-5} level for light gluino scenarios, which might lead an observable event rate around 1.8. Should the integrated luminosity increase at later runs of LHC, one could obtain larger event rates (up to 10 events) if the flavor violation is driven by the up squark sector. If the flavor violation comes from the down sector of the unconstrained MSSM, the event rate remains below the observable level.

For the single top production case $pp \rightarrow t\bar{c} + \bar{t}c + X$, we already included cuts for the transverse momentum and rapidity of the charm and top quarks in the final state, as well as a lower cut for jet separation. In this case, if assume that the top quark is going to be reconstructed in the final state one can predict, for example, 50 000 events for an

⁹Considering the W decay hadronically would produce a 6 jet final state, requiring determination of the multijet trigger threshold.

integrated luminosity 100 fb^{-1} and $\sigma(pp \rightarrow t\bar{c} + X) = 0.5 \text{ pb}$. A similar total efficiency consideration will go to reduce this further but there exist enough events to find a signal under the best-case scenario. Anything beyond the above qualitative discussion about the observability of the decay and production channels will be considered in more detail in our future paper [27].

V. CONCLUSION

In this study we analyzed two related issues in top quark physics. In the first part of the paper, we concentrated on the comparison of two rare top quark decays, $t \rightarrow cgg$ versus $t \rightarrow cg$, within the unconstrained MSSM, driven by mixing between the second and third generations only. To the best of our knowledge, $t \rightarrow cgg$ decay has been considered only in our recent study [9] within the SM framework, where $\text{BR}(t \rightarrow cgg)$ was found to be 2 orders of magnitude larger than $\text{BR}(t \rightarrow cg)$. However, in the SM, $\text{BR}(t \rightarrow cgg)$ remains at 10^{-9} level, and thus too small to be detectable. Any experimental signature of such channel would require the existence of physics beyond the SM which justifies further analyses. Here we studied this decay in the MSSM framework by allowing nonzero flavor off-diagonal parameters. Our conclusion of the dominance of the branching ratio of $t \rightarrow cgg$ over $t \rightarrow cg$ in the SM paper remains mostly valid in the MSSM framework, but now the BR's can become as large as 10^{-6} – 10^{-5} .¹⁰ For the cases in which we impose the GUT relation between gaugino masses and assume a flavor violation in down squark sector, the large difference in ratio between the $t \rightarrow cgg$ and $t \rightarrow cg$ modes disappears only in the case of very large intergenerational flavor-violating parameters (close to 1, or to their maximally allowed upper values). In that case, $t \rightarrow cg$ exceeds $t \rightarrow cgg$. In the case of nonzero $(\delta_{U,D}^{23})_{AB}$, $t \rightarrow cg$ dominates $t \rightarrow cgg$, except in regions of small flavor violation. Once we relax the GUT constraints, there is no longer such a large difference between the two and three body decays, as long as a small flavor violation is turned on. Once the flavor off-diagonal parameters, $(\delta_{U,D}^{23})_{AB}$, are introduced, the difference in branching ratios disappears as the parameters are minute and $\text{BR}(t \rightarrow cg)$ becomes around 5 times larger than $\text{BR}(t \rightarrow cgg)$. As expected, if the SUSY-GUT relations hold, both modes cannot exceed 10^{-7} level (except for flavor violating parameters near their maximum allowed values for $t \rightarrow cg$ decay), because the gluino mass is large. Once we relax this condition, both $t \rightarrow cgg$ and $t \rightarrow cg$ have branching ratios of the order 10^{-6} – 10^{-5} and 10^{-5} , respectively.

Having shown that the three body rare decay $t \rightarrow cgg$ is indeed important (comparable with, or larger than, the two body decay $t \rightarrow cg$), we carried out a complete calculation of the single top-charm associated production at LHC via gluon fusion at partonic level within the same scenarios

discussed above. This production cross section has been considered before including only the SUSY-QCD contributions [8]. We performed a complete analysis by including all the electroweak contributions: the chargino-down-type squark, neutralino-up-type squark, charged Higgs, as well as the SM contributions. For simplification, a common SUSY FCNC parameter δ is assumed, $(\delta_{U,D}^{23})_{LL} = (\delta_{U,D}^{23})_{RR} = (\delta_{U,D}^{23})_{LR} = (\delta_{U,D}^{23})_{RL}$ (in the up and down squark sectors), but most often only one common δ parameter in either sector is allowed to be nonzero each time. We have shown that, in the most promising scenarios (if a common SUSY FCNC parameter δ is assumed), the total hadronic cross section $\sigma(pp \rightarrow t\bar{c} + \bar{t}c + X)$ can become as large as 50–60 fb and could reach a few hundred fb, especially if we relax the GUT relations between the gaugino masses and assume a flavor violation from one sector only (LL, LR, RL, or RR). We have shown that the cross section could be as large as 600–700 fb if a large flavor violation coming from only $(\delta_U^{23})_{LR}$ is allowed.

The comparative gluino, chargino and other contributions to the process have been estimated. The gluino contributions dominate over most of the parameter space, when allowing flavor violation in both up and down squark mass matrices to be of the same order of magnitude. However, the chargino contribution is non-negligible and would be dominant in either the constrained MSSM, or if the flavor violation was allowed to be much larger in the down than in the up squark sector. While the chargino loop is 2 orders of magnitude smaller than the gluino for $(\delta_U^{23})_{AB} = (\delta_D^{23})_{AB}$, the contribution of the “rest” (neutralino, charged Higgs and SM) is around half of the chargino contribution, for all of the SUSY FCNC parameters chosen.

Gluon fusion could be more promising than $cg \rightarrow t$, $q\bar{q} \rightarrow t\bar{c}$, or $cg \rightarrow gt$, which we leave for a further study [27].

The huge differences in prediction between the constrained and the unconstrained MSSM scenarios make LHC a fertile testing ground for the study of SUSY FCNC processes. Any significant rate for the top-charm associated production would be a signal of physics beyond the SM, and, in particular, of new flavor physics.

ACKNOWLEDGMENTS

The work of M. F. was funded by NSERC of Canada (SAP0105354). The work of G. E. was supported in part by the Israel Science Foundation and by the Fund for the Promotion of Research at the Technion. G. E. would like to thank J. J. Cao for helpful discussions. I. T. would like to thank Micheal Rauch for his help and suggestions about the use of the HADCALC program.

Note added.—After submitting the first version of the present paper to the archive (hep-ph/0601253.v1) we became aware of an analysis similar to ours: [28]. They analyze the QCD SUSY contribution, and take as flavor

¹⁰The cutoff parameter $C = 0.1$ is being used.

violation only $(\delta_{\bar{U}}^{23})_{LL} \neq 0$, while we switched all flavor violating parameters on between the second and third generations. In our analysis a nonzero $(\delta_{\bar{U}}^{23})_{LR}$ parameter

is dominant (by one order of magnitude over $(\delta_{\bar{U}}^{23})_{LL}$), which makes a comparison of our results to theirs difficult.

-
- [1] For a recent review, see: A. Taffard (CDF and D0 Collaborations), Report No. FERMILAB-CONF-05-494-E Proceedings of the Hadron Collider Physics Symposium 2005, Les Diablerets, Switzerland, 2005.
- [2] See e.g.: Z. Sullivan, Phys. Rev. D **70**, 114012 (2004), and references therein.
- [3] Q. H. Cao, R. Schwienhorst, and C. P. Yuan, Phys. Rev. D **71**, 054023 (2005); Q. H. Cao, R. Schwienhorst, J. A. Benitez, R. Brock, and C. P. Yuan, Phys. Rev. D **72**, 094027 (2005); J. Campbell and F. Tramontano, Nucl. Phys. **B726**, 109 (2005); J. Campbell, R. K. Ellis, and F. Tramontano, Phys. Rev. D **70**, 094012 (2004); Q. H. Cao and C. P. Yuan, Phys. Rev. D **71**, 054022 (2005), and references therein.
- [4] Z. Sullivan, Phys. Rev. D **72**, 094034 (2005); O. Cakir and S. A. Cetin, J. Phys. G **31**, N1 (2005).
- [5] T. Han, R. D. Peccei, and X. Zhang, Nucl. Phys. **B454**, 527 (1995); T. Tait and C. P. Yuan, Phys. Rev. D **55**, 7300 (1997); J. Cao, G. Eilam, K. i. Hikasa, and J. M. Yang, Phys. Rev. D **74**, 031701 (2006).
- [6] E. Malkawi and T. Tait, Phys. Rev. D **54**, 5758 (1996); T. Han, M. Hosch, K. Whisnant, B. L. Young, and X. Zhang, Phys. Rev. D **58**, 073008 (1998); Y. P. Gouz and S. R. Slabospitsky, Phys. Lett. B **457**, 177 (1999); A. Belyaev and N. Kidonakis, Phys. Rev. D **65**, 037501 (2002); P. M. Ferreira, O. Oliveira, and R. Santos, Phys. Rev. D **73**, 034011 (2006); P. M. Ferreira and R. Santos, Phys. Rev. D **73**, 054025 (2006).
- [7] C. S. Li, X. Zhang, and S. H. Zhu, Phys. Rev. D **60**, 077702 (1999); H. Zhou, W. G. Ma, Y. Jiang, R. Y. Zhang, and L. H. Wan, Phys. Rev. D **64**, 095006 (2001); H. Zhou, W. G. Ma, and R. Y. Zhang, hep-ph/0208170; C. X. Yue, Y. B. Dai, Q. J. Xu, and G. L. Liu, Phys. Lett. B **525**, 301 (2002); J. J. Cao, Z. H. Xiong, and J. M. Yang, Phys. Rev. D **67**, 071701(R) (2003); Nucl. Phys. **B651**, 87 (2003).
- [8] J. J. Liu, C. S. Li, L. L. Yang, and L. G. Jin, Nucl. Phys. **B705**, 3 (2005).
- [9] G. Eilam, M. Frank, and I. Turan, Phys. Rev. D **73**, 053011 (2006).
- [10] F. Gabbiani, E. Gabrielli, A. Masiero, and L. Silvestrini, Nucl. Phys. **B477**, 321 (1996); M. Misiak, S. Pokorski, and J. Rosiek, Adv. Ser. Dir. High Energy Phys. **15**, 795 (1998); M. Ciuchini, E. Franco, A. Masiero, and L. Silvestrini, Phys. Rev. D **67**, 075016 (2003); **68**, 079901 (2003).
- [11] R. Harnik, D. T. Larson, H. Murayama, and A. Pierce, Phys. Rev. D **69**, 094024 (2004).
- [12] T. Besmer, C. Greub, and T. Hurth, Nucl. Phys. **B609**, 359 (2001); D. A. Demir, Phys. Lett. B **571**, 193 (2003); A. M. Curiel, M. J. Herrero, and D. Temes, Phys. Rev. D **67**, 075008 (2003); J. J. Liu, C. S. Li, L. L. Yang, and L. G. Jin, Nucl. Phys. **B705**, 3 (2005).
- [13] J. L. Lopez, D. V. Nanopoulos, and R. Rangarajan, Phys. Rev. D **56**, 3100 (1997); G. M. de Divitiis, R. Petronzio, and L. Silvestrini, Nucl. Phys. **B504**, 45 (1997); S. Bejar, J. Guasch, and J. Sola, in Proc. of the 5th International Symposium on Radiative Corrections (RADCOR 2000), edited by Howard E. Haber; hep-ph/0101294; J. J. Cao, Z. H. Xiong, and J. M. Yang, Nucl. Phys. **B651**, 87 (2003).
- [14] L. J. Hall, V. A. Kostelecky, and S. Raby, Nucl. Phys. **B267**, 415 (1986); A. Masiero and L. Silvestrini, in *Perspectives on Supersymmetry*, edited by G. Kane (World Scientific, Singapore, 1998).
- [15] M. Frank and I. Turan, Phys. Rev. D **72**, 035008 (2005).
- [16] T. Hahn and M. Perez-Victoria, Comput. Phys. Commun. **118**, 153 (1999); T. Hahn, Nucl. Phys. B, Proc. Suppl. **89**, 231 (2000); Comput. Phys. Commun. **140**, 418 (2001); T. Hahn and C. Schappacher, Comput. Phys. Commun. **143**, 54 (2002); T. Hahn, hep-ph/0506201.
- [17] M. Rauch, HADCALC (unpublished).
- [18] C. Greub and P. Liniger, Phys. Rev. D **63**, 054025 (2001).
- [19] G. Passarino and M. J. G. Veltman, Nucl. Phys. **B160**, 151 (1979).
- [20] R. Mertig and J. Kublbeck, Prepared for International Workshop on Software Engineering, Artificial Intelligence and Expert Systems for High-energy and Nuclear Physics, Lyon, France, 1990; J. Kublbeck, H. Eck, and R. Mertig, Nucl. Phys. B, Proc. Suppl. **29**, 204 (1992).
- [21] S. Eidelman *et al.* (Particle Data Group), Phys. Lett. B **592**, 1 (2004).
- [22] S. Heinemeyer, W. Hollik, and G. Weiglein, Comput. Phys. Commun. **124**, 76 (2000); S. Heinemeyer, W. Hollik, and G. Weiglein, Eur. Phys. J. C **9**, 343 (1999); G. Degrassi, S. Heinemeyer, W. Hollik, P. Slavich, and G. Weiglein, Eur. Phys. J. C **28**, 133 (2003); T. Hahn, S. Heinemeyer, W. Hollik, and G. Weiglein, hep-ph/0507009.
- [23] M. Peskin and D. Schroeder, *An Introduction to Quantum Field Theory* (Addison-Wesley, Reading, MA, 1995).
- [24] W. Giele *et al.*, hep-ph/0204316.
- [25] J. Pumplin, A. Belyaev, J. Huston, D. Stump, and W. K. Tung, J. High Energy Phys. **02** (2006) 032.
- [26] Brigitte Vachon (private communication).
- [27] J. Cao, G. Eilam, M. Frank, I. Turan, and J. M. Yang (unpublished).
- [28] J. Guasch, W. Hollik, S. Penaranda, and J. Sola, Nucl. Phys. B, Proc. Suppl. **157**, 152 (2006).